Supplementary Information for

A tandem activity-based sensing and labeling strategy reveals antioxidant response element regulation of labile iron pools

Aidan T. Pezacki[a,1], Ryan L. Gonciarz[b,1], Toshitaka Okamura[a], Carson D. Matier[a], Laura Torrente[c], Ke Cheng[b], Sophia Miller[d], Martina Ralle[d], Nathan P. Ward[c], Gina M. DeNicola[c], Adam R. Renslo[b,e,2], Christopher J. Chang[a,f,g,2]

[a]Department of Chemistry, University of California, Berkeley, CA 94720; [b]Department of Pharmaceutical Chemistry, University of California, San Francisco, CA 94158; [c]Department of Metabolism and Physiology, H. Lee Moffitt Cancer Center and Research Institute, Tampa, FL 33612; [d]Department of Molecular and Medical Genetics, Oregon Health & Science University, Portland, OR 97239; [e]Helen Diller Family Comprehensive Cancer Center, University of California, San Francisco, CA 94158; [f]Department of Molecular and Cell Biology, University of California, Berkeley, CA 94720; and [g]Helen Wills Neuroscience Institute, University of California, Berkeley, CA 94720

[1]These authors contributed equally

[2]Corresponding Authors: *E-mail: adam.renslo@ucsf.edu; chrischang@berkeley.edu

This PDF includes:

1. General Methods

Chemical Reagents and Materials. All chemical reagents were obtained commercially and used without further purification, unless otherwise stated. Anhydrous solvents were purchased from Sigma-Aldrich and were used without further purification. Solvents used for flash column chromatography and reaction workup procedures were purchased from either Sigma-Aldrich or Fisher Scientific. Column chromatography was performed on Silicycle Sili-prep cartridges using a Biotage Isolera Four automated flash chromatography system. Instrumentation. **RhoNox-4** was purchased from Dojindo as FerroOrange (F374). **TRX-Puro** was prepared as described previously (1) and immunostaining was performed with mouse Anti-puromycin purchased from Kerafast (Kf-Ab02366-1.1) and anti-mouse secondary antibody Alexa Fluor™ 488 purchased from Invitrogen (A-21202).

Spectroscopic Methods. NMR spectra were recorded on either a Varian INOVA 400 MHz spectrometer (with 5 mm QuadNuclear Z-Grad Probe), calibrated to $CH(D)Cl_3$ as an internal reference (7.27 and 77.00 ppm for 1 H and 13C NMR spectra, respectively) or a Bruker Shield Plus 600 MHz spectrometer. Data for 1H NMR spectra are reported in terms of chemical shift (δ, ppm), multiplicity, coupling constant (Hz), and integration. Data for ^{13}C NMR spectra are reported in terms of chemical shift (δ, ppm), with multiplicity. The following abbreviations are used to denote the multiplicities: s = singlet, d = doublet, t = triplet, q = quartet, m = multiplet, br = broad, app = apparent, or combinations thereof. Compound purity was determined using a Waters Acquity QDa mass spectrometer equipped with FTN-H Sample Manager, Evaporative Light Scattering Detector and Photodiode Array Detector. Separations were carried out with Acquity UPLC® BEH C18, 1.7mm, 2.1 x 50 mm column, at 25 °C using a mobile phase of water-acetonitrile containing a constant 0.05% formic acid. HPLC was performed on a Waters 2535 Separation Module with a Waters 2998 Photodiode Array Detector using an XBridge BEH C18, 3.5µm, 4.6 x 20 mm column, at ambient temperature (unregulated) using a mobile phase of water-methanol containing a constant 0.05% formic acid. High-resolution mass spectra (HRMS) were obtained using a Xevo G2-XS QTof Quadrupole Time-of-Flight Mass Spectrometer. All compounds synthesized were ≥95% pure as determined by ^{1}H NMR and UPLC-MS. Fluorescence spectra were measured using a PTI QuantaMaster 400 fluorimeter (Horiba). Reaction trace monitoring was carried out using an Agilent 1260 Infinity II System with an InfinityLab LC/MSD XT (column: EC-C18, 120 Å, 2.7 µm, 4.6 x 100 mm, method: 0 to 8 minutes 5% to 100% MeCN with 0.1% FA in H_2O with 0.1% FA, 8 to 12 minutes hold at 100% MeCN with 0.1% FA, flow rate 1.500 mL/min).

Photophysical Properties. A stock solution of **IG1** (60 μM), **3-O-Methylfluorescein** (10 μM), **IG1-FM** (60 μM), and **FI-CH_2OH** (10 μM) were prepared in PBS (corning, 21-040-CV). A stock solution of fluorescein (2.5 μM) was prepared in 0.1 N NaOH. The absorbance spectrum for each fluorophore was then measured followed by the fluorescence emission spectrum (λ_{ex} = 475 nm, 488 nm for fluorescein, λ_{em} = 500-650 nm). The wavelength of maximum absorbance and emission were recorded. A serial

dilution was then performed for each fluorophore (**IG1** = 45, 22.5, 11.25, 0 μM; **3-O-Methylfluorescein** = 5, 2.5, 1.25, 0 μM; **IG1-FM** = 40, 20, 10, 0 μM; **FI-CH_2OH** = 5, 2.5, 1.25, 0 μM; fluorescein = 1.25, 0.625, 0.3125, 0 μM) and the absorbance and emission spectra of the diluted samples were recorded. The area under the curve was calculated for all emission spectra using Prism9 (GraphPad). For each fluorophore, the integrated fluorescence intensity was plotted against the maximum absorbance for the various probe concentrations, and the quantum yield was calculated from the slope normalized to the slope and quantum yield of fluorescein (Φ = 0.92). The extinction coefficient was calculated via the Beer–Lambert law.

Metal Selectivity Analysis. **IG1-FM** was dissolved in DMSO to obtain a 100 μM stock solution. The stock solution of **IG1-FM** was then diluted (1 μM) in 50 mM HEPES (pH = 7.4) and preincubated for 5 minutes. Then, various metal ions (1 mM NaCl, 1 mM KCl, 1 mM $CaCl_2$, 1 mM $MgCl_2$, 1 mM $MnCl_2$, 10 μM $(NH_4)_2Fe(SO_4)_2$, 10 μM $FeCl_3$, 10 μM $CoSO_4$, 10 μM $NiCl_2$, 10 μM CuCl, 10 μM $CuSO_4$, 10 μM $CuSO_4$, or 10 μM $ZnSO_4$) or biologically relevant molecules (10 μM myoglobin, 1 mM H_2O_2, or 1 mM GSH) were added such that the total volume was equal to 1 mL and incubated at 37 °C for various times. The fluorescence spectra of **IG1-FM** were collected with an emission window between 500 nm to 650 nm and excitation at 488 nm (step size = 1 nm, integration = 0.5 seconds).

***In Vitro* Protein Labeling. IG1-FM** (1, 5, or 10 μM) and HSA (0.5 mg/mL) were incubated at 25 °C for 30 minutes with or without $(NH_4)_2Fe(SO_4)_2$ (10, 50, 100 μM respectively). The final volume was 50 μL. The solution mixture was mixed with NuPAGE® LDS Sample Buffer (4X) and heated at 37 °C for 10 minutes, followed by separation on Novex tris-glycine gels (Invitrogen) and scanned by ChemiDoc MP (Bio-Rad Laboratories, Inc) for measuring in-gel fluorescence. The fluorescence of **IG1-FM** was measured by 530/28 nm band pass filter with excitation using blue epi-illumination. After that, the total protein level on the gel was assayed by Coomassie brilliant blue (CBB) solution (Bio Rad; 161-0400) according to the manufacturer's protocol and scanned by ChemiDoc MP. Protein labeling on cell lysate was fulfilled similarly. To prepare cell lysates, HEPG2 cells were cultured in a 6-well plate to 80% confluency. The cells were then rinsed twice with PBS, scraped off the plate, centrifuged (0.3 G at 4 °C for 10 minutes), and resuspended in RIPA lysis buffer (Boston BioProducts; BP-116X) with cOmplete™ ULTRA Tablets, EDTA-free Protease Inhibitor Cocktail (Roche; 05892953001). The lysate was then centrifuged (12 G at 4 °C for 20 minutes) and the supernatant was collected, and the protein concentrations were measured by Pierce™ Detergent Compatible Bradford Assay Kit (Thermo-Fisher; 23246). **IG1-FM** (5, 10, or 25 μM) and HEPG2 cell lysate (1.0 mg/mL) were incubated at 25 °C for 2 hours with or without $(NH_4)_2Fe(SO_4)_2$ (50, 100, 250 μM respectively). The final volume was 50 μL. The solution mixture was mixed with NuPAGE® LDS Sample Buffer (4X) and heated at 37 °C for 10 minutes, followed by separation on Novex tris-glycine gels (Invitrogen) and scanned by ChemiDoc MP (Bio-Rad Laboratories, Inc) for measuring in-gel fluorescence.

Cell Culture. Cells were maintained by the UC Berkeley Tissue Culture Facility. HEPG2 cells were maintained as a monolayer in exponential growth at 37 °C in a 5% CO_2 atmosphere in DMEM, low glucose, GlutaMAX™ Supplement, pyruvate (DMEM, Gibco) supplemented with 10% fetal bovine serum (FBS, Seradigm). WT and KO HeLa cells, and KO A549 cells were maintained as a monolayer in exponential growth at 37 °C in a 5% CO_2 atmosphere in DMEM, high glucose, GlutaMAX™ Supplement, pyruvate (DMEM, Gibco) supplemented with 10% FBS. H1975, H1299, PC-9, H460, and H1944 cells were maintained as a monolayer in exponential growth at 37 °C in a 5% CO_2 atmosphere in RPMI 1640, L-Glutamine (RPMI, Gibco) supplemented with 10% FBS. Two to three days before imaging, cells were passed and plated on an 8-well chamber slide (Ibidi µ-Slide 8 Well). For HEPG2 cells, chamber slides were coated with poly L-lysine prior to plating (50 mg/mL, Sigma, St. Louis, MO).

Cell Viability Assay. Hoechst 33342 was used to confirm cell viability upon treatment with **IG1-FM** and iron supplementation/chelation. HEPG2 cells were plated at 30% confluency in a 96-well plate in low glucose DMEM/10% FBS. Cells were incubated with 100 µL of vehicle control or 250 µM DFO for 24 hours. Medium was then replaced with vehicle control or 100 µM FAS in low glucose DMEM/10% FBS for 90 minutes, washed once with HBSS (+Ca, Mg), incubated with 5 µM **IG1-FM** in HBSS for 1 h, washed twice with HBSS, and then incubated with 500 nM Hoechst 33342 for 15 minutes. Fluorescence was then read on a plate reader (monofilter) with λ_{ex} = 350 nm (9 mm bandwidth), λ_{em} = 460 (9 mm bandwidth), 15 mm plate height and top-down fluorescence detection.

Confocal Fluorescence Imaging. HEPG2 cells were seeded at 30% confluency in a poly L-lysine coated 8-well chamber slide (Ibidi) and allowed to grow to 70% confluency before performing cell imaging. HEPG2 cells were incubated with vehicle control, 250 µM DFO, or 4 µg/mL Hepcidin in low glucose DMEM/10% FBS for 24 hours. Medium was then replaced with vehicle control or 100 µM FAS in low glucose DMEM/10% FBS for 90 minutes, washed once with HBSS (+Ca, Mg) and incubated with 5 µM **IG1-FM** in HBSS with 1% DMSO for 1 hour. Cells were washed twice with HBSS and then imaged. HeLa cells were seeded at 30% confluency in an 8-well chamber slide (Ibidi) and were allowed to grow to 70% confluency before performing cell imaging. HeLa cells were incubated with vehicle control or 50 µM FAC in DMEM/10% FBS for 24 h. Medium was then replaced with vehicle control or 100 µM DFO in DMEM/10% FBS for 24 h, washed once with HBSS (+Ca, Mg), incubated with 5 µM **IG1-FM** with 1% DMSO in HBSS for 1 h, and then imaged. NRF2 KO A549, H1975, H1299, PC-9, H460, and H1944 cells were seeded at 30% confluency in an 8-well chamber slide (Ibidi) and were allowed to grow to 70% confluency before performing cell imaging. H1975, H1299, PC-9, H460, and H1944 cells were incubated with vehicle control or 1 µM KI-696 in RPMI 1640/10% FBS for 48 hours. Cells were washed once with HBSS (+Ca, Mg) and incubated with 5 µM **IG1-FM** with 1% DMSO in HBSS for 1 h and then imaged. **RhoNox-4** treated cells were stained for 30 minutes in HBSS (1 µM with 1% DMSO) and washed twice with HBSS prior to imaging. Confocal fluorescence imaging of all cell lines was performed with a Zeiss laser scanning microscope LSM880 with a 20x dry objective lens using Zen 2015 software (Carl Zeiss,

Zen 2.3 black). **IG1-FM** was excited using a 488 nm diode laser and emission was collected using a META detector between 495 to 625 nm. **RhoNox-4** was excited using a 561 nm diode laser and emission was collected using a META detector between 570 to 630 nm.

Puromycin Immunofluorescence. H1975, H1299, PC-9, H460, and H1944 cells were seeded at 30% confluency in an 8-well chamber slide (Ibidi) and were allowed to grow to 70% confluency before performing cell imaging. Cells were incubated with vehicle control or 1 μM KI-696 in RPMI 1640/10% FBS for 48 hours. Cells were then washed twice with RPMI (no FBS) and incubated with 1 μM **TRX-Puro** or puromycin in RPMI (no FBS) for 4 h at 37 ^{o}C with 5% CO_2. Cells were washed once with PBS, fixed with 4% paraformaldehyde for 10 minutes at room temperature, and washed twice with PBS. The solution was then replaced with 0.1% Triton X-100 in PBS and incubated for 10 minutes at room temperature. The solution was replaced with a primary anti-puromycin antibody solution (1:500 vol/vol with 10% FBS and 0.1% Triton X-100 in PBS) and incubated for 30 minutes at 37 ^{o}C. The cells were washed three times with 0.1% Triton X-100 in PBS and then incubated with a secondary antibody–Alexa Fluor™ 488 conjugate solution (1:100 vol/vol with 1 μM Hoechst 33342, 10% FBS, and 0.1% Triton X-100 in PBS) for 30 minutes at 37 ^{o}C. Cells were then washed three times with PBS and imaged via confocal fluorescence microscopy (See Confocal Fluorescence Imaging methods section). Alexa Fluor™ 488 was excited using a 488 nm diode laser and emission was collected using a META detector between 495 to 625 nm. Hoechst 33342 was excited using a 405 nm diode laser and emission was collected using a META detector between 425 to 495 nm.

Inductively Coupled Plasma-Mass Spectrometry (ICP-MS). Cell pellets containing approximately 10^6 cells were digested in 50 μl of concentrated HNO_3 (trace metal grade, Thermo Fisher Scientific). The samples were digested by heating to 90°C for 1 hour loosely capped in a heating block. After digestion, 1% HNO_3 (trace metal grade, Thermo Fisher Scientific) was added to each sample for a final volume of 2 mL, followed by an additional 2x dilution in 1% HNO_3. ICP-MS analysis was performed using an Agilent 8900 triple quad equipped with an SPS autosampler. The system was operated at a radio frequency power of 1550 W, an argon plasma gas flow rate of 15 L/min, and an Ar carrier gas flow rate of 0.9 L/min. The data was quantified using weighed, serial dilutions of a multi-element standard (CEM 2, VHG Labs, VHG-SM70B-100) and a single element standard for P (SpexCertiPrep PLP9-2Y). A solution of NIST SRM 1683f was prepared at 8x dilution in 1% HNO_3 and measured to ensure accuracy of the calibration curve. Three bovine liver standards (NIST SRM 1577c) were measured to ensure accurate elemental recovery, prepared by the same method that was used for the samples. An internal standard (Sc, Ge, Bi) continuously introduced with the sample was used to correct for detector fluctuations and to monitor plasma stability. Each sample was acquired in biological triplicates and averaged.

RNA Extraction and RNA Sequencing Analysis. H1975 cells were treated with vehicle (DMSO) or 100 nM KI-696 for 60 hours. RNA extraction was performed using the RNeasy

plus mini kit (Qiagen, catalog #74134). Prior to RNA sequencing, RNA quality was verified by Qubit in the Moffitt Tissue Core and all samples had a RIN > 9.5. Additional RNA QC, sequencing, mapping to the human genome, normalization including fragments per kilobase per million mapped fragments (FPKM) and differential expression analyses were performed by Novogene.

Cell Death Assay. Cells were plated in 96-well plates at a density of 2,500 – 4,000 cells/well (final volume = 100 µL). The next day, the medium was changed to 100 µl of RPMI 1640 containing 20 nM of Sytox Green, as previously described (2). The number of dead cells and cell confluency were measured by a CellCyte X (Cytena, Freiburg im Breisgau, Germany) at 37°C with 5% CO_2. Data were acquired with a 10X objective lens in phase contrast and green fluorescence channels (Ex/Em: 460/524 nm, acquisition time: 200 ms). Images were acquired from each well at 6-hour intervals. Image and data processing were performed with CellCyte Studio software (Cytena). Dead cell number was normalized to cell confluency [Number of Sytox Green positive cells/mm^2/cell confluency (% of total image)]. Relative cell death was determined via the area under the curve of DFO-treated cells / the area under the curve of control cells. Each measurement was performed in biological triplicates and averaged.

Image Analysis and Quantification. Fiji (National Institutes of Health) was used for image analysis. The area of stained cells was selected by setting the appropriate threshold with a Gaussian blur filter (sigma = 1). The “Create Mask” function followed by the “Create Selection” function were then used to create a selection from this threshold. Using this selection, the mean fluorescence was measured. For each biological replicate, four images in different fields of cells were analyzed and the values were combined for statistical analysis. Statistical comparison of **IG1-FM** fluorescence in different conditions versus control was performed using an unpaired t-test (assume Gaussian distribution, no Welch’s correction) in Prism9 (GraphPad). For representative confocal images, the maximum and minimum brightness was kept consistent for all images.

2. Synthesis of Iron Probes

(1″-R, 3″-R)-Dispiro[adamantane2,3'- [1,2,4]trioxolane-5′,1″-cyclohexan]-3″-yl (2-((chlorocarbonyl)(methyl)amino)ethyl)(methyl)carbamate (2)

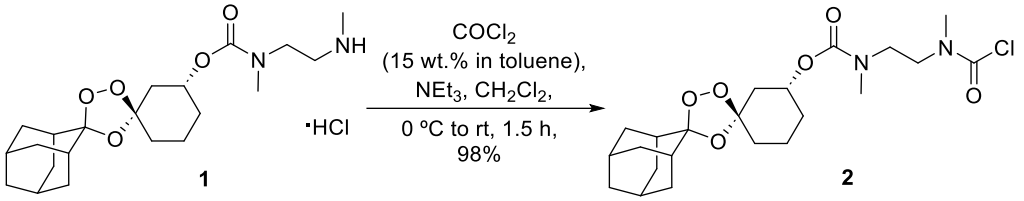

To an Ar(g) purged vial containing amine **1** synthesized as reported previously (3) in anhydrous CH_2Cl_2 (5 mL), was added phosgene (15 wt. % in toluene) (8.74 mL, 12.3 mmol, 33.0 equiv) and the mixture cooled to 0 °C. NEt_3 (103 µL, 0.74 mmol, 2.0 equiv) was added dropwise and the mixture stirred at 0 °C for 1.5 h. Upon completion, the reaction was carefully concentrated *in vacuo* with 5 M aq. NaOH solution in the receiving flask to quench unreacted phosgene (**Caution:** phosgene is highly toxic). The crude residue was subjected to azeotropic distillation with toluene (3 × 5 mL) and purified via flash column chromatography (12 g silicycle column, 0-30 % EtOAc–Hexanes) to afford the title compound **2** (166.6 mg 0.365 mmol, 98%) as a colorless semi-solid. ^{1}H NMR (400 MHz, $CDCl_3$) δ 4.83 – 4.69 (m, 1H), 3.71 – 3.46 (m, 3H), 3.46 – 3.30 (m, 1H), 3.12 (app. dd, *J* = 34.3, 9.0 Hz, 3H), 2.93 (app. d, *J* = 12.5 Hz, 3H), 2.29 – 2.17 (m, 1H), 2.01 – 1.87 (m, 7H), 1.87 – 1.67 (m, 11H), 1.65 – 1.44 (m, 2H), 1.43 – 1.29 (m, 1H); ^{13}C NMR (100 MHz, $CDCl_3$) 155.9, 155.7, 155.3, 155.2, 150.2, 149.7, 148.9, 111.6, 108.7, 108.6, 71.8, 71.7, 71.7, 71.6, 50.7, 50.4, 49.4, 48.4, 46.8, 46.7, 46.0, 45.9, 41.2, 40.0, 39.9, 39.6, 38.9, 37.6, 37.1, 36.7, 36.3, 35.8, 35.1, 34.9, 34.8, 34.7, 34.6, 34.5, 34.0, 33.9, 30.7, 30.6, 26.9, 26.4, 25.8, 19.7, 19.6; HRMS (ESI) (calcd for $C_{22}H_{33}ClN_2O_6$ $[M + Na]^+$: m/z 479.1919 found: 479.1941.

(1″-R, 3″-R)-Dispiro[adamantane2,3'- [1,2,4]trioxolane-5′,1″-cyclohexan]-3″-yl (5'-formyl-3'-methoxy-3-oxo-3H-spiro[isobenzofuran-1,9'-xanthen]-6'-yl) ethane-1,2-diylbis(methylcarbamate) (3)

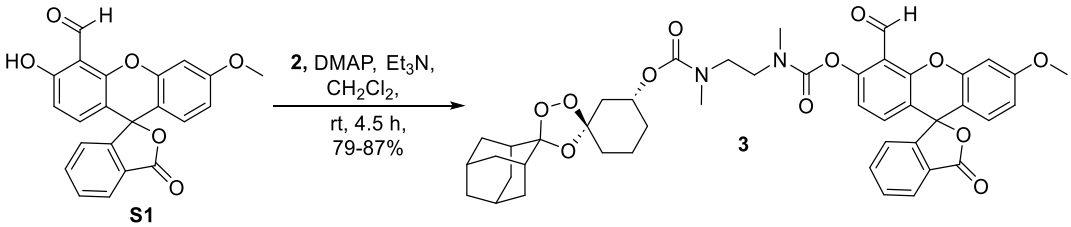

To a solution of carbamoyl chloride **2** (60.0 mg, 0.13 mmol, 1.0 equiv) in CH_2Cl_2 (2 mL) was added NEt_3 (27.5 uL, 0.20 mmol, 1.5 equiv) and DMAP (19.2 mg, 0.16 mmol, 1.2 equiv). The reaction was stirred for 10 mins at rt before formyl fluorescein **S1** (59.0 mg, 0.16 mmol, 1.2 equiv) was added and the reaction stirred at rt for 4.5 h. Upon completion,

the mixture was concentrated *in vacuo*, resuspended in EtOAc (30 mL) and sonicated to aid dissolution. Deionized water (30 mL) was added and the layers were separated. The organic phase was washed with a mixture of DI water (7 × 30 mL) and brine (ca. 2 mL each wash) to aid phase separation, followed by a final brine wash (1 × 50 mL). The organic phase was then dried ($MgSO_4$), filtered and concentrated under reduced pressure to a crude residue. Purification via flash column chromatography (12 g silicycle column, 0-50 % EtOAc–Hexanes, product eluted at 50% EtOAc) afforded the title compound **3** (91.0 mg, 0.11 mmol, 87%) as a colorless solid. ^{1}H NMR (400 MHz, $CDCl_3$) δ 10.75 (s, 1H), 8.05 (d, *J* = 7.4 Hz, 1H), 7.68 (dt, *J* = 15.0, 7.5 Hz, 2H), 7.19 (t, *J* = 8.2 Hz, 1H), 7.03 (d, *J* = 8.6 Hz, 1H), 6.94 – 6.83 (m, 2H), 6.76 – 6.66 (m, 2H), 4.85 – 4.71 (m, 1H), 3.86 (s, 3H), 3.79 – 3.35 (m, 4H), 3.21 – 3.03, (m, 3H), 3.00 – 2.92, (m, 3H), 2.29 – 2.17 (m, 1H), 2.01 – 1.78 (m, 11H), 1.75 – 1.60 (m, 8H), 1.55 – 1.45 (m, 1H), 1.42 – 1.32 (m, 1H); ^{13}C NMR (100 MHz, $CDCl_3$) δ 187.0, 186.9, 169.0, 161.7, 155.9, 155.7, 155.4, 155.4, 153.9, 153.8, 153.6, 153.4, 152.5 (multiple peaks), 152.4 (multiple peaks), 152.1, 152.1, 151.9, 151.5 135.4, 134.4, 134.2, 134.1, 130.2, 129.0, 126.3, 125.3, 124.0, 119.5, 119.4, 117.7 (multiple peaks), 117.6, 117.0 (multiple peaks), 112.8, 111.6, 110.6, 108.7, 108.6, 101.0, 81.6, 71.5, 71.4, 71.4, 55.7, 47.7, 47.6, 47.5, 47.1, 46.7 (multiple peaks), 46.6, 46.3, 46.2, 40.1, 39.9, 36.7, 36.3, 35.7, 35.5, 35.1, 34.9, 34.8, 34.7, 34.6, 34.5, 34.0 (multiple peaks), 30.8 (multiple peaks), 26.9, 26.4, 19.6; HRMS (ESI) calcd for $C_{44}H_{47}N_2O_{12}$ $[M + H]^+$: m/z 795.3124 found: 795.3074. Additional peaks in the ^{1}H and ^{13}C-NMR spectrum of compound **3** are attributed to the slow interconversion of *N,N'*-dimethylethylene-diamine rotamers on the NMR timescale. The use of VT-NMR to coalesce rotameric resonances was not possible due to instability of **3** at elevated temperatures.

(1″-R, 3″-R)-Dispiro[adamantane2,3'- [1,2,4]trioxolane-5′,1″-cyclohexan]-3″-yl (5'-(hydroxymethyl)-3'-methoxy-3-oxo-3H-spiro[isobenzofuran-1,9'-xanthen]-6'-yl) ethane-1,2-diylbis(methylcarbamate) (4)

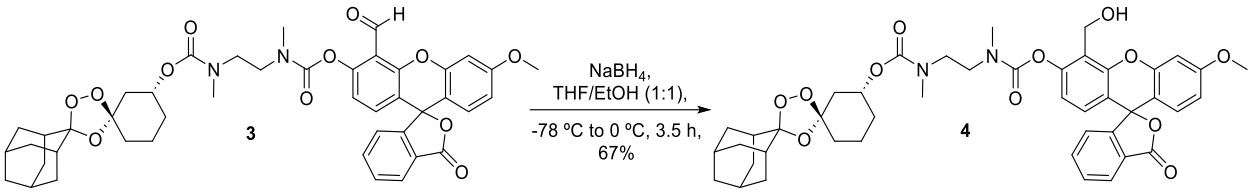

To a solution of aldehyde **3** in THF/EtOH (1:1) (4 mL) at -78 °C, was added $NaBH_4$ (7.0 mg, 0.19 mmol, 1.6 equiv) and the reaction stirred at -78 °C for 3 h and then 0 °C for 30 min. Upon completion, the reaction was quenched with satd. aq. NH_4Cl (15 mL) and extracted with EtOAc (30 mL). The aqueous layer was back-extracted with EtOAc (3 × 20 mL) and the combined organic phases were dried ($MgSO_4$), filtered and concentrated *in vacuo* to a crude residue. Purification via flash column chromatography (12 g silicycle column, 0-50 % EtOAc–Hexanes, product eluted at 50% EtOAc) afforded the title

compound **4** (91.0 mg, 0.11 mmol, 87%) as a colorless solid. ^{1}H NMR (400 MHz, $CDCl_3$) δ 8.04 (d, *J* = 7.4 Hz, 1H), 7.66 (dt, *J* = 20.8, 7.3 Hz, 2H), 7.20 (d, *J* = 7.3 Hz, 1H), 6.91 (s, 1H), 6.87 – 6.75 (m, 2H), 6.75 – 6.69 (m, 1H), 6.65 (dd, *J* = 8.8, 2.5 Hz, 1H), 4.96 – 4.73 (m, 3H), 3.86 (s, 3H), 3.77 – 3.32 (m, 4H), 3.13 (app. d, *J* = 48.5 Hz, 3H), 3.01 – 2.90 (m, 3H), 2.59 (br s, 1H), 2.29 – 2.17 (m, 1H), 2.02 – 1.79 (m, 11H), 1.76 – 1.59 (m, 8H), 1.57 – 1.47 (m, 1H), 1.41 – 1.31 (m, 1H); ^{13}C NMR (100 MHz, $CDCl_3$) δ 169.3, 161.5, 156.1, 153.1 (multiple peaks), 152.9 (multiple peaks), 152.7, 152.2, 150.9, 150.8 (multiple peaks), 150.6 (multiple peaks), 150.5, 135.1, 129.9, 128.9, 128.7, 128.5 (multiple peaks), 128.4, 126.5, 125.1, 124.1, 121.9 (multiple peaks), 121.7, 117.9, 117.8, 117.1, 112.5, 111.6, 110.7, 108.7, 108.6, 100.9, 82.7, 71.9, 71.6, 55.7, 54.3, 54.2, 54.1, 54.0, 47.5 (multiple peaks), 47.1 (multiple peaks), 47.0, 46.6, 46.2, 46.0, 40.0, 39.9, 39.8, 36.7, 36.3, 35.4, 34.9, 34.8, 34.7, 34.7, 34.3, 34.0, 33.9, 30.7 (multiple peaks), 29.7, 26.9, 26.4, 19.6 (multiple peaks), 19.5; HRMS (ESI) calcd for $C_{44}H_{49}N_2O_{12}$ $[M + H]^+$: m/z 797.3280 found: 797.3349. Additional peaks in the ^{1}H and ^{13}C-NMR spectrum of compound **4** are attributed to the slow interconversion of *N,N'*-dimethylethylene-diamine rotamers on the NMR timescale. The use of VT-NMR to coalesce rotameric resonances was not possible due to instability of **4** at elevated temperatures.

(1″-R, 3″-R)-Dispiro[adamantane2,3'- [1,2,4]trioxolane-5',1″-cyclohexan]-3″-yl (5'-(fluoromethyl)-3'-methoxy-3-oxo-3H-spiro[isobenzofuran-1,9'-xanthen]-6'-yl) ethane-1,2-diylbis(methylcarbamate) (Iron Green-1 Fluoromethyl, IG1-FM)

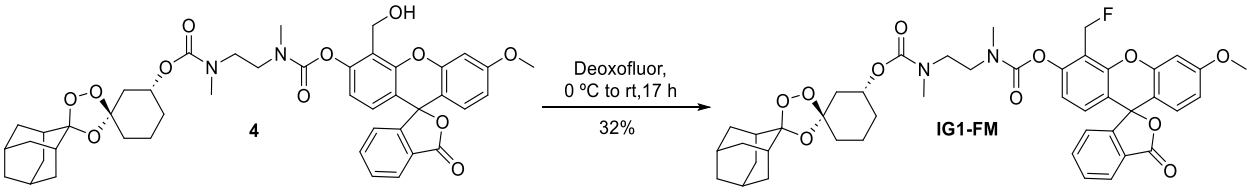

To a solution of alcohol **4** (60.5 mg, 0.07 mmol, 1.0 equiv) in anhydrous CH_2Cl_2 (4 mL) at 0 °C was added Deoxo-Fluor (bis(2-methoxyethyl)aminosulfur trifluoride, 50 wt. %) 2.7 M in toluene (33.5 µL, 0.09 mmol, 1.4 equiv) and the reaction gradually warmed to rt for 5 h. The reaction was then cooled to 0 °C before an additional portion of Deoxo-Fluor (50 wt. %) 2.7 M in toluene (33.5 µL, 0.09 mmol, 1.4 equiv) was added and the reaction warmed to rt and stirred for 12 h. The following day, the reaction was quenched with deionized water (25 mL) and the layers separated. The aqueous layer was back-extracted with CH_2Cl_2 (3 × 25 mL) and the combined organic phases dried ($MgSO_4$), filtered and concentrated *in vacuo*. The crude residue was purified via preparative HPLC (75-85% MeCN–water) to afford the title compound **IG1-FM** (16.7 mg, 0.02 mmol, 32%) as a colorless solid. ^{1}H NMR (400 MHz, $CDCl_3$) δ 8.05 (d, *J* = 7.4 Hz, 1H), 7.74 – 7.61 (m, 2H), 7.19 (t, *J* = 6.5 Hz, 1H), 6.97 – 6.84 (m, 3H), 6.73 (d, *J* = 8.8 Hz, 1H), 6.67 (dd, *J* = 8.9, 2.4 Hz, 1H), 5.77 (q, *J* = 10.9 Hz, 1H), 5.65 (q, *J* = 11.3 Hz, 1H), 4.79 (br. s, 1H), 3.88 (s, 3H), 3.71 – 3.36 (m, 4H), 3.23 – 3.04 (m, 3H), 3.00 – 2.91 (m, 3H), 2.28 – 2.21 (m, 1H),

2.02 – 1.72 (m, 15H), 1.64 – 1.45 (m, 4H), 1.39 – 1.30 (m, 2H); ^{13}C NMR (151 MHz, $CDCl_3$) δ 169.2, 161.6, 155.9, 155.4, 154.0, 153.5, 152.8 (multiple peaks), 152.1 (multiple peaks), 152.0, 150.6, 135.1, 129.9, 128.9, 126.5, 125.1, 124.1, 118.3 (multiple peaks), 118.1 (multiple peaks), 116.6, 116.4 (multiple peaks), 116.3, 112.4, 111.6, 110.8, 108.6, 100.9, 82.4, 74.3, 73.2, 71.7, 71.6, 71.5, 55.7, 47.5, 47.4 (multiple peaks), 47.0 (multiple peaks), 46.7, 46.1 (multiple peaks), 40.1, 39.9, 36.8, 36.3, 35.6, 35.6, 35.4, 35.3, 34.9, 34.8, 34.7, 34.7, 34.3, 34.0, 30.7 (multiple peaks), 29.7, 29.3, 26.9, 26.5, 19.7, 19.6; ^{19}F NMR (376 MHz, $CDCl_3$) δ -210.3, -210.4, -210.5, -211.0, -211.0, -211.1, -215.1; HRMS (ESI) calcd for $C_{44}H_{48}FN_2O_{11}$ $[M + H]^+$: m/z 799.3237 found: 799.3303; Additional peaks in the ^{1}H, ^{13}C and ^{19}F-NMR spectrum of **IG1-FM** are attributed to the slow interconversion of *N,N'*-dimethylethylene-diamine rotamers on the NMR timescale. The use of VT-NMR to coalesce rotameric resonances was not possible due to instability of **IG1-FM** at elevated temperatures.

Tert-butyl (3'-methoxy-3-oxo-3H-spiro[isobenzofuran-1,9'-xanthen]-6'-yl) ethane-1,2-diylbis(methylcarbamate) (7)

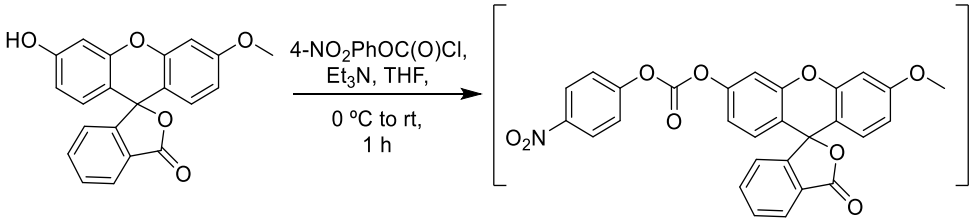

To an Ar(g) purged flask containing 3-O-methylfluorescein **5** (50.0 mg, 0.144 mmol, 1.0 equiv) and anhydrous THF (6 mL) cooled to 0 °C was added 4-nitrophenyl chloroformate (29.1 mg, 0.144 mmol, 1.0 equiv) and triethylamine (101 uL, 0.722 mmol, 5.0 equiv). The reaction was gradually warmed to room temperature for 1 h. Formation of carbonate intermediate **6** was confirmed by UPLC-MS (ESI) (calcd for $C_{28}H_{18}NO_9$ $[M + H]^+$: m/z 512.10 found: 512.18) and the reaction was cooled to 0 °C before *tert*-butyl methyl(2-(methylamino)ethyl)carbamate (136 mg, 0.722 mmol, 5.0 equiv) was added dropwise. The reaction was stirred for 15 min at 0 °C until UPLC-MS confirmed complete consumption of the carbonate intermediate **6**. The reaction was concentrated, resuspended in Et_2O (8 mL) and washed with satd. aq $NaHCO_3$ (7 × 10 mL), brine (1 × 50 mL), dried (MgSO4) and concentrated to a crude residue. Purification via flash column chromatography (12 g silicycle column, 0-50 % EtOAc–Hexanes) afforded the title

compound **7** (36.6 mg, 0.065 mmol, 45%) as a colorless solid. ^{1}H NMR (400 MHz, $CDCl_3$) δ 8.03 (d, *J* = 7.5 Hz, 1H), 7.72 – 7.59 (m, 2H), 7.18 (dd, *J* = 7.5, 4.8 Hz, 1H), 7.11 (dd, *J* = 5.7, 2.2 Hz, 1H), 6.87 – 6.75 (m, 3H), 6.74 – 6.68 (m, 1H), 6.63 (dd, *J* = 8.8, 2.5 Hz, 1H), 3.85 (s, 3H), 3.57 (br s, 1H), 3.48 (br s, 3H), 3.10 (app. br d, *J* = 33.6 Hz, 3H), 2.97 – 2.90 (m, 3H), 1.44 – 1.52 (m, 9H); ^{13}C NMR (100 MHz, $CDCl_3$) δ 169.4, 161.4, 155.6 (multiple peaks), 154.1 (multiple peaks), 153.9, 153.1, 153.1, 152.7, 152.4, 151.9, 151.8, 135.1, 129.8, 129.0, 128.9, 128.8, 126.5, 125.0, 124.1, 124.1, 117.7, 117.5, 116.2, 116.0, 111.8, 111.0, 110.5 (multiple peaks), 110.3, 100.9, 82.6, 80.0, 79.7, 55.6, 53.8, 47.2 (multiple peaks), 35.3, 34.6, 29.3, 28.5; MS (ESI) calcd for $C_{31}H_{33}N_2O_8$ $[M + H]^+$: m/z 561.22, found: 561.35. Additional peaks in the ^{1}H and ^{13}C-NMR spectrum of compound **7** are attributed to the slow interconversion of N-Boc and/or *N,N'*-dimethylethylene-diamine rotamers on the NMR timescale. The use of VT-NMR to coalesce rotameric resonances was not possible due to instability of **7** at elevated temperatures.

3'-Methoxy-3-oxo-3H-spiro[isobenzofuran-1,9'-xanthen]-6'-yl methyl(2-(methylamino)ethyl)carbamate trifluoroacetic acid salt (8)

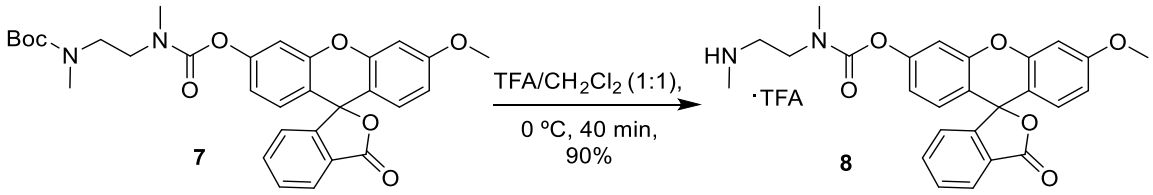

To a solution of intermediate **7** (36.5 mg, 0.07 mmol, 1.0 equiv) in CH_2Cl_2 (2.80 mL), cooled to 0 °C, was added TFA (2.80 mL) and the mixture stirred at 0 °C for 40 min. Upon completion, the reaction was concentrated under reduced pressure and subjected to azeotropic distillation with toluene (3 × 5 mL). The crude residue was resuspended in Et_2O (3 × 10 mL) and reconcentrated several times with sonication to afford the title compound **8** (33.8 mg, 0.06 mmol, 90%) as a light yellow solid, which was sufficiently pure to be used in the next step without further purification. MS (ESI) calcd for $C_{26}H_{24}N_2O_6Na$ $[M + Na]^+$: m/z 483.15 found: 483.26.

(1″-R, 3″-R)-Dispiro[adamantane2,3'- [1,2,4]trioxolane-5',1″-cyclohexan]-3″-yl (3'-methoxy-3-oxo-3H-spiro[isobenzofuran-1,9'-xanthen]-6'-yl) ethane-1,2-

diylbis(methylcarbamate) (Iron Green-1, IG1)

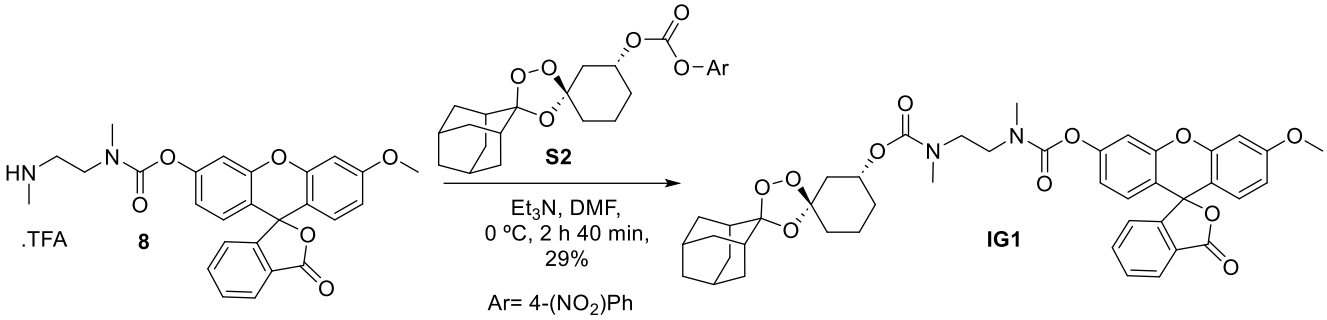

To an Ar(g) purged vial containing (*R,R*)-dispiro[adamantane-2,3'-[1,2,4]trioxolane-5',1''-cyclohexan]-3''-yl (4-nitrophenyl) carbonate **S2** synthesized as previously reported (4) (32.5 mg, 0.073 mmol, 1.0 equiv) was added anhydrous DMF (1.2 mL) and Et_3N (25.4 µL, 0.182 mmol, 2.5 equiv). The mixture was cooled to 0 °C before amine **8** (16.8 mg, 36.5 µmol, 0.5 equiv) was added and the reaction maintained at 0 °C for 1 h until an additional portion of amine **8** (16.8 mg, 36.5 µmol, 0.5 equiv) was added. The reaction was stirred at 0 °C for a total of 2 h 40 min before benzyl amine (8 uL, 0.07 mmol, 1.3 equiv) was added to react remaining carbonate **S2** and aid product separation. The reaction was stirred for an additional 15 min at rt before EtOAc (30 mL) and deionized water (20 mL) were added and the layers separated. The organic phase was washed with deionized water (4 × 20 mL), brine (1 × 30 mL), dried ($MgSO_4$) and concentrated *in vacuo* to a crude semi-solid. Purification via preparative HPLC (30-100% MeCN–water) afforded the title compound **IG1** (13.2 mg, 0.017 mmol, 29%) as a colorless solid. ^{1}H NMR (400 MHz, $CDCl_3$) δ 8.04 (d, *J* = 7.3 Hz, 1H), 7.75 – 7.60 (m, 2H), 7.23 – 7.14 (m, 1H), 7.11 (s, 1H), 6.88 – 6.76 (m, 3H), 6.72 (d, *J* = 8.8 Hz, 1H), 6.64 (dd, *J* = 8.8, 2.5 Hz, 1H), 4.86 – 4.74 (m, 1H), 3.86 (s, 3H), 3.74 – 3.23 (m, 4H), 3.02 – 3.20 (m, 3H), 3.01 – 2.91 (m, 3H), 2.33 – 2.22 (m, 1H), 2.05 – 1.70 (m, 16H), 1.68 – 1.45 (m, 4H), 1.45 – 1.31 (m, 1H); ^{13}C NMR (100 MHz, $CDCl_3$) δ 169.4, 161.4, 155.9, 155.7 (multiple peaks), 155.4 (multiple peaks), 154.3, 154.1, 153.9, 153.1 (multiple peaks), 153.1, 152.8 (multiple peaks), 152.6 (multiple peaks), 152.4, 151.9, 151.8, 135.1, 129.8, 129.0, 128.9 (multiple peaks), 126.6, 126.5, 125.1, 124.1, 117.7, 117.6, 116.3, 116.2 (multiple peaks), 116.1, 111.9, 111.6, 111.0, 110.4, 110.3 (multiple peaks), 108.7, 100.9, 82.6, 71.7 (multiple peaks), 71.4 (multiple peaks), 69.5, 55.6, 53.8, 47.5, 47.3, 47.0 (multiple peaks), 46.8, 46.7, 46.1, 40.1 (multiple peaks), 39.9, 36.8, 36.3, 35.5, 35.4, 35.2, 35.1, 34.9, 34.8, 34.7, 34.6, 34.4, 34.1, 33.9, 31.8, 30.8 (multiple peaks), 30.7 (multiple peaks), 29.7, 29.3, 26.9, 26.4, 19.7, 19.6; HRMS (ESI) calcd for $C_{43}H_{47}N_2O_{11}$ $[M + H]^+$: m/z 767.3174, found: 767.3290. Additional peaks in the ^{1}H and ^{13}C-NMR spectrum of **IG1** are attributed to the slow interconversion of *N,N'*-dimethylethylene-diamine rotamers on the NMR timescale. The use of VT-NMR to coalesce rotameric resonances was not possible due to instability of **IG1** at elevated temperatures.

3. SI Figures

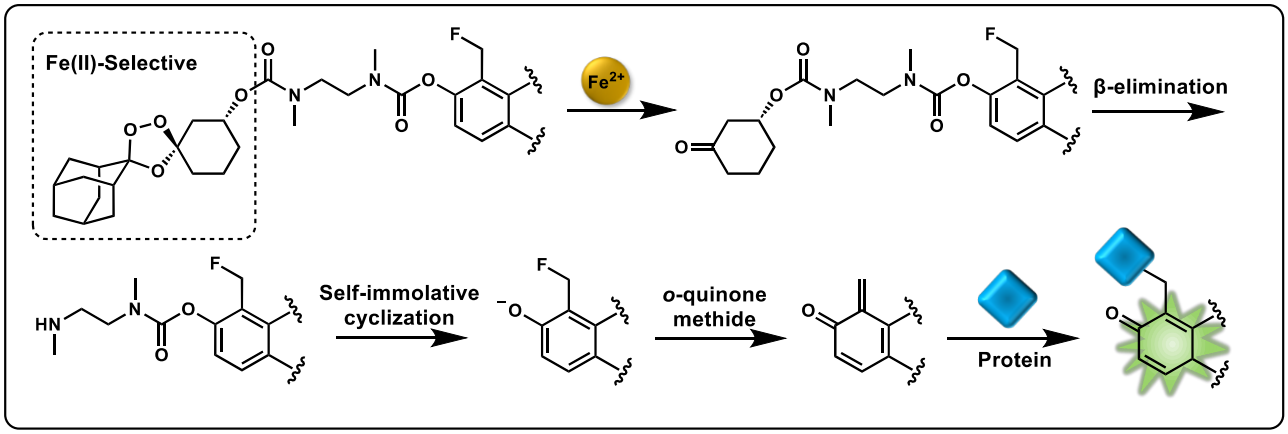

Scheme S1. Proposed fragmentation cascade and bioconjugation of **IG1-FM** in the presence of ferrous iron.

Table S1. Photophysical properties of **IG1**, **IG1-FM**, and their representative reaction products **3-O-Methylfluorescein** and **Fl-CH_2OH**, respectively.

	λ_{abs} (nm)	λ_{em} (nm)	ε ($M^{-1}cm^{-1}$)	Φ
IG1	475	515	655	0.023
3-O-Methylfluorescein	475	512	30233	0.29
IG1-FM	475	515	1494	0.015
Fl-CH_2OH	475	520	24396	0.15

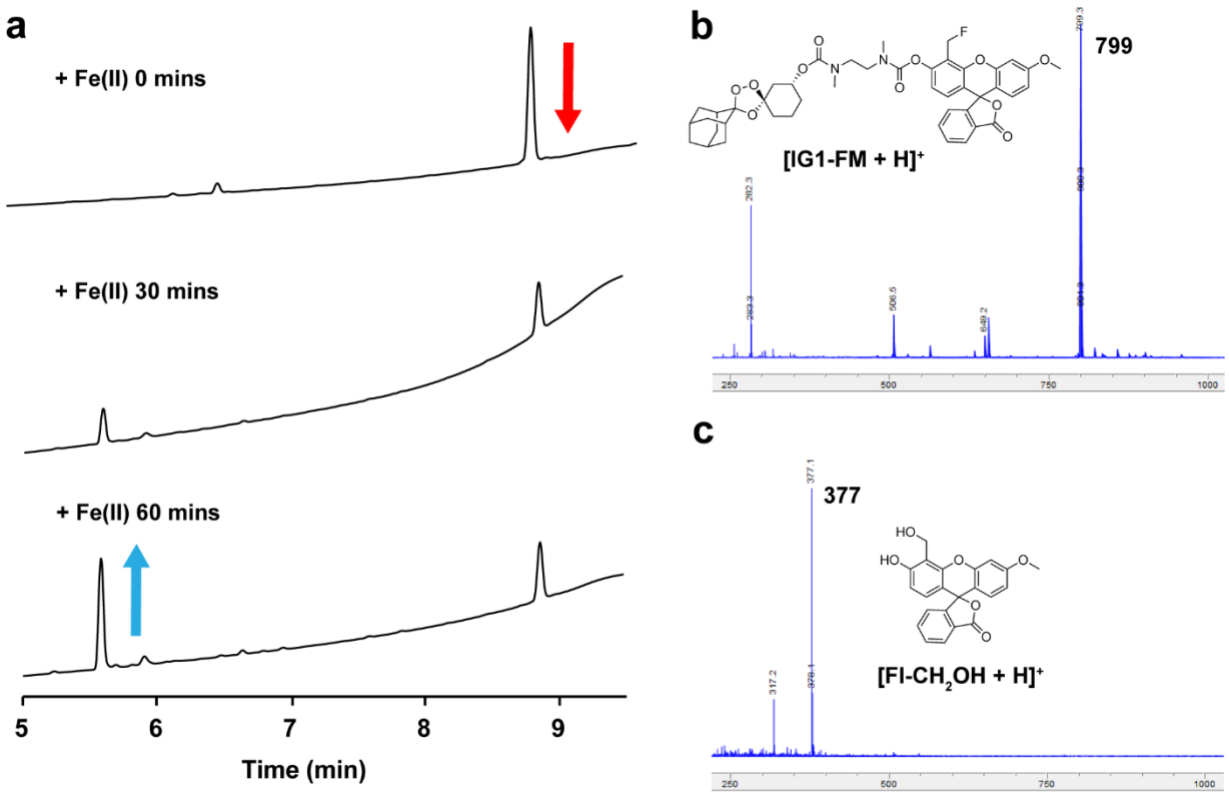

Figure S1. Liquid chromatography (LC) chromatograms of the reaction between **IG1-FM** and Fe(II). 100 μM **IG1-FM** was added to a solution of 200 μM $(NH_4)_2Fe(SO_4)_2$ and 1 mM GSH in 25 mM HEPES with (pH = 7.4) and the mixture was incubated at 37 ^oC for 1 hour. Signal traces were measured via absorbance at 250 nm. (B) The mass of intact **IG1-FM** was detected at a retention time of 9 min. (C) The hydrolyzed product of **IG1-FM**, hydroxymethyl fluorescein (Fl-CH_2OH), is detected at a retention time of 5.6 min. Fl-CH_2OH is obtained by TRX-cleavage, linker immolation, and quenching of the quinone methide by water.

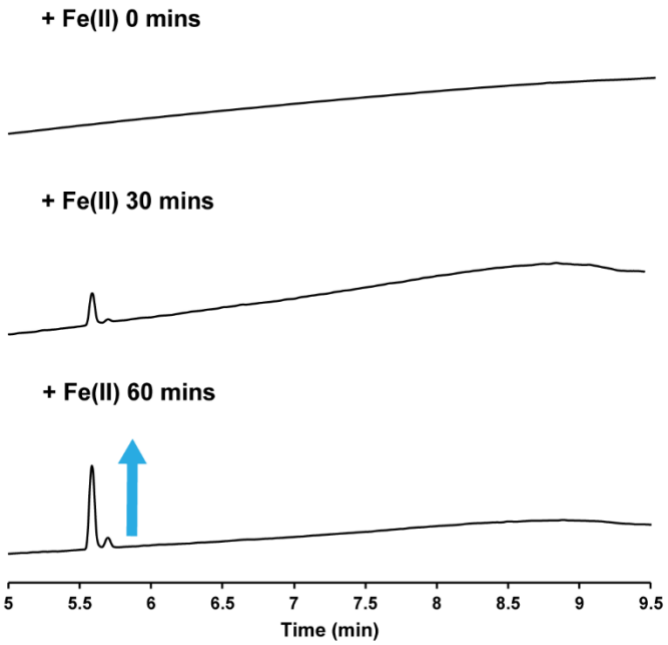

Figure S2. LC chromatograms of the reaction between **IG1-FM** and Fe(II). Signal traces were measured via absorbance at 488 nm. Fl-CH_2OH, is detected at a retention time of 5.6 min.

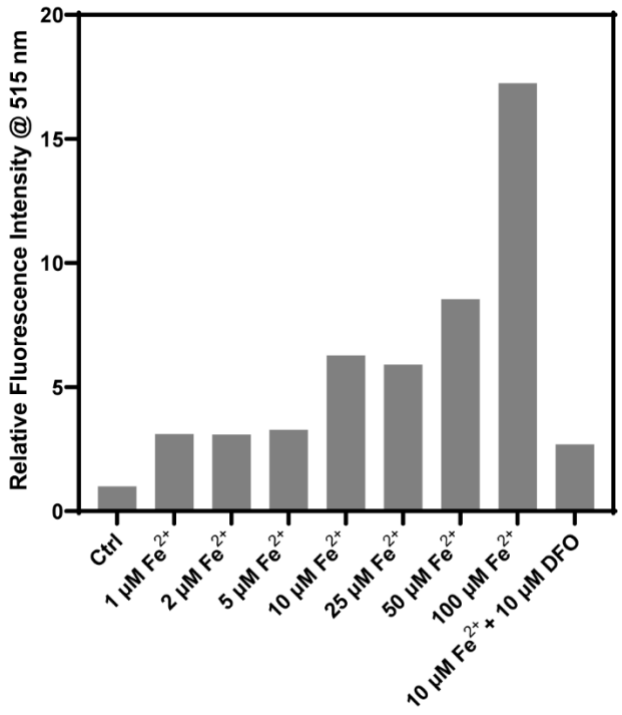

Figure S3. Dose dependence of 1 μM **IG1-FM** in response to varying amounts of Fe. **IG1-FM** was incubated with 0 to 100 equivalents of Fe at 37 °C in 50 mM HEPES (pH 7.4) for 1 h and then fluorescence emission was collected at 515 nm (λ_{ex} = 488 nm).

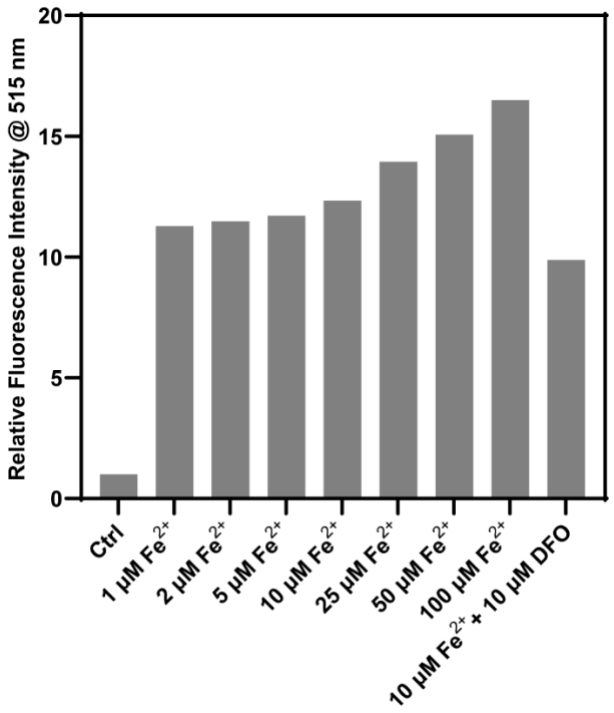

Figure S4. Dose dependence of 1 μM **IG1** in response to varying amounts of Fe. **IG1** was incubated with 0 to 100 equivalents of Fe at 37 °C in 50 mM HEPES (pH 7.4) for 1 h prior to fluorescence emission collection at 515 nm (λ_{ex} = 488 nm).

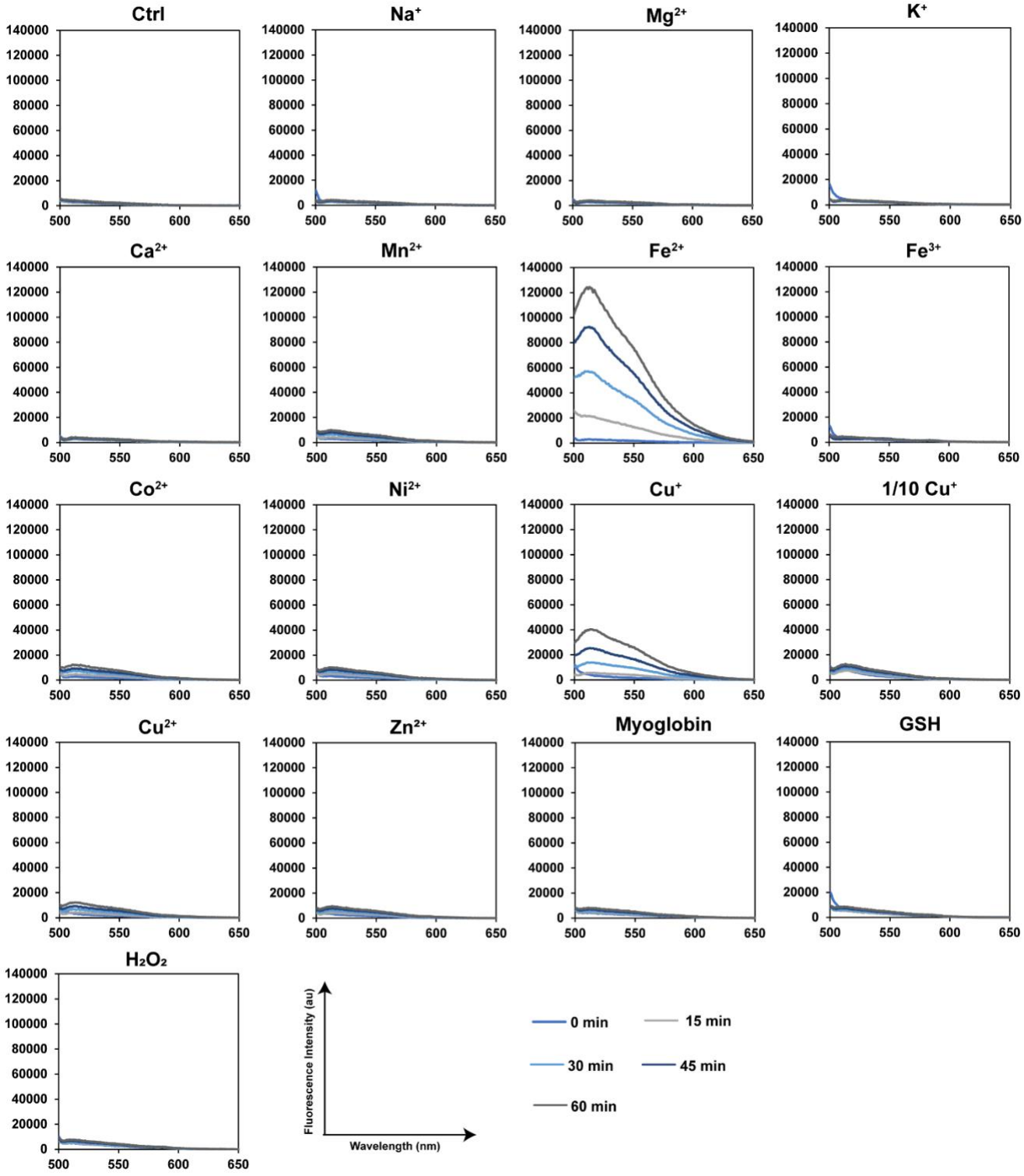

Figure S5. Fluorescence emission spectra of 1 μM **IG1-FM** reacted with various biologically relevant s-block (1 mM) and d-block (10 μM) metals, myoglobin (10 μM), glutathione (GSH, 1 mM), and H_2O_2 (1 mM). Measurements were acquired at 37 °C in HEPES (pH 7.4) using a fluorimeter at 0, 5, 15, 30, 45, and 60 min.

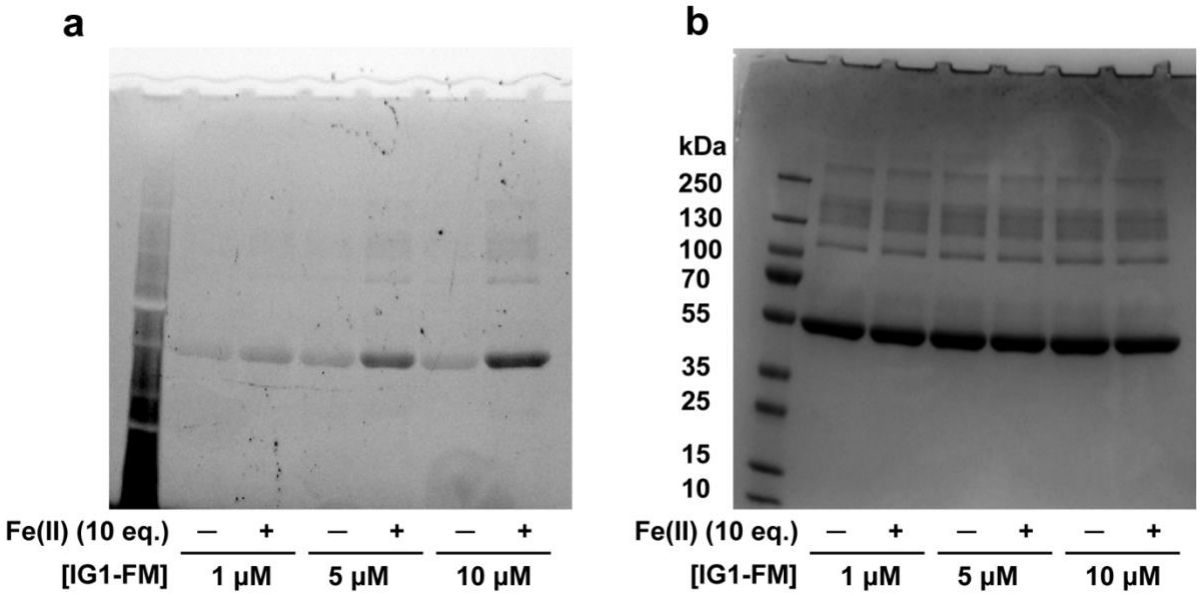

Figure S6. Full images of SDS–PAGE analysis on human serum albumin (HSA) treated with various concentrations of **IG1-FM** with and without 10 equivalents of Fe(II). (a) Protein labeling by **IG1-FM**, as measured by in-gel fluorescence. (b) HSA concentration, as measured by Coomassie stain.

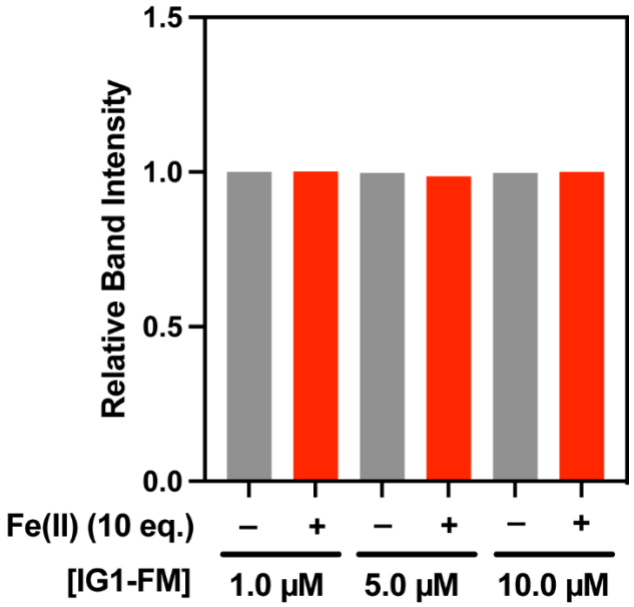

Figure S7. Quantified concentration of human serum albumin (HSA) treated with various concentrations of **IG1-FM** with and without 10 equivalents of Fe(II), as measured by Coomassie stain. In-gel band intensity was scanned by ChemiDoc MP and signal intensity was analyzed by Image Lab.

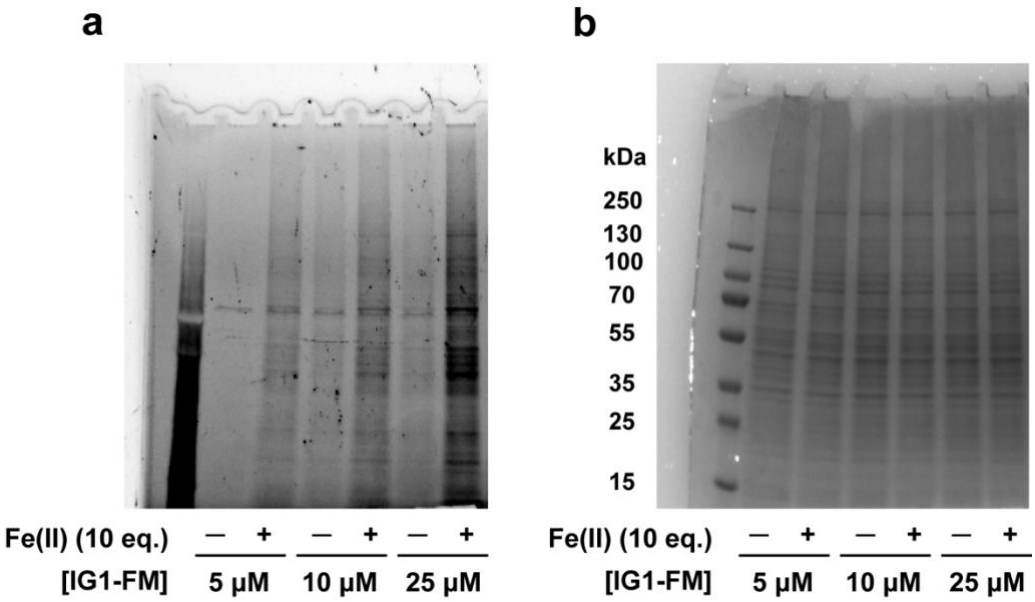

Figure S8. Full images of SDS–PAGE analysis on HEPG2 cell lysate treated with various concentrations of **IG1-FM** with and without 10 equivalents of Fe(II). (a) Protein labeling by **IG1-FM**, as measured by in-gel fluorescence. (b) HEPG2 cell lysate concentration, as measured by Coomassie Stain.

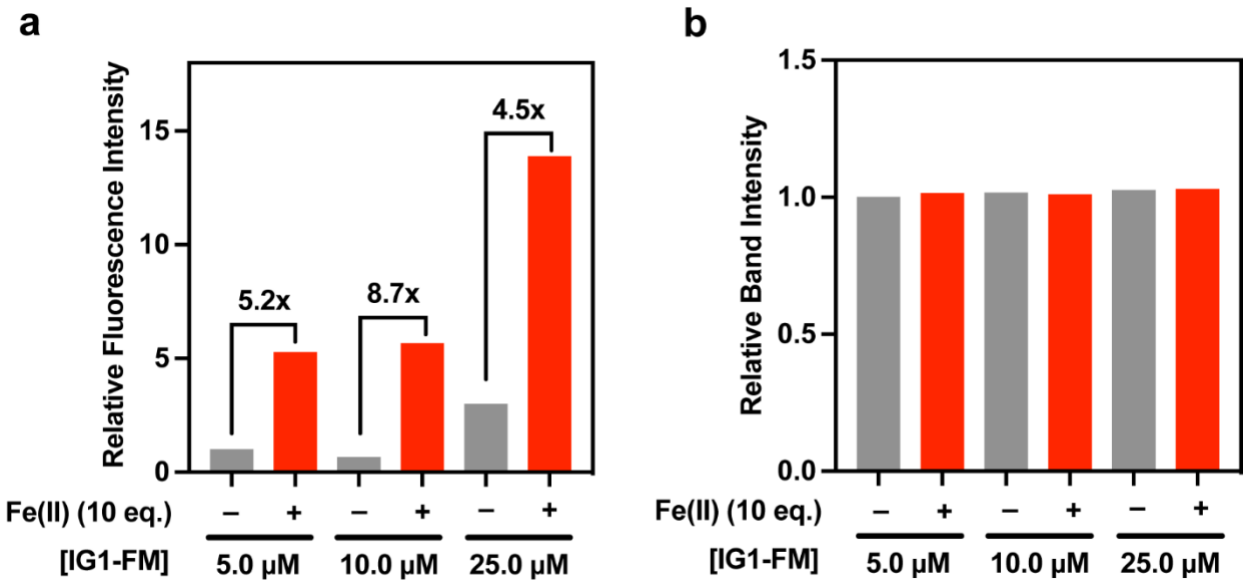

Figure S9. Fe(II)-dependent protein labeling of **IG1-FM** in HEPG2 cell lysate. (a) Quantified fluorescence intensities of HEPG2 cell lysate treated with various concentrations of **IG1-FM** with and without 10 equivalents of Fe(II). A solution of HEPG2 cell lysate (1.0 mg/mL) and **IG1-FM** (5-25 μM) in 50 mM HEPES (pH 7.4) was incubated with or without Fe(II) (10 eq.) for 2 h. Protein labeling was measured by total lane fluorescence intensity. (b) Quantified concentration of HEPG2 cell lysate, as measured by Coomassie stain. In-gel fluorescence/intensity for SDS-PAGE was scanned by ChemiDoc MP and signal intensity was analyzed by Image Lab.

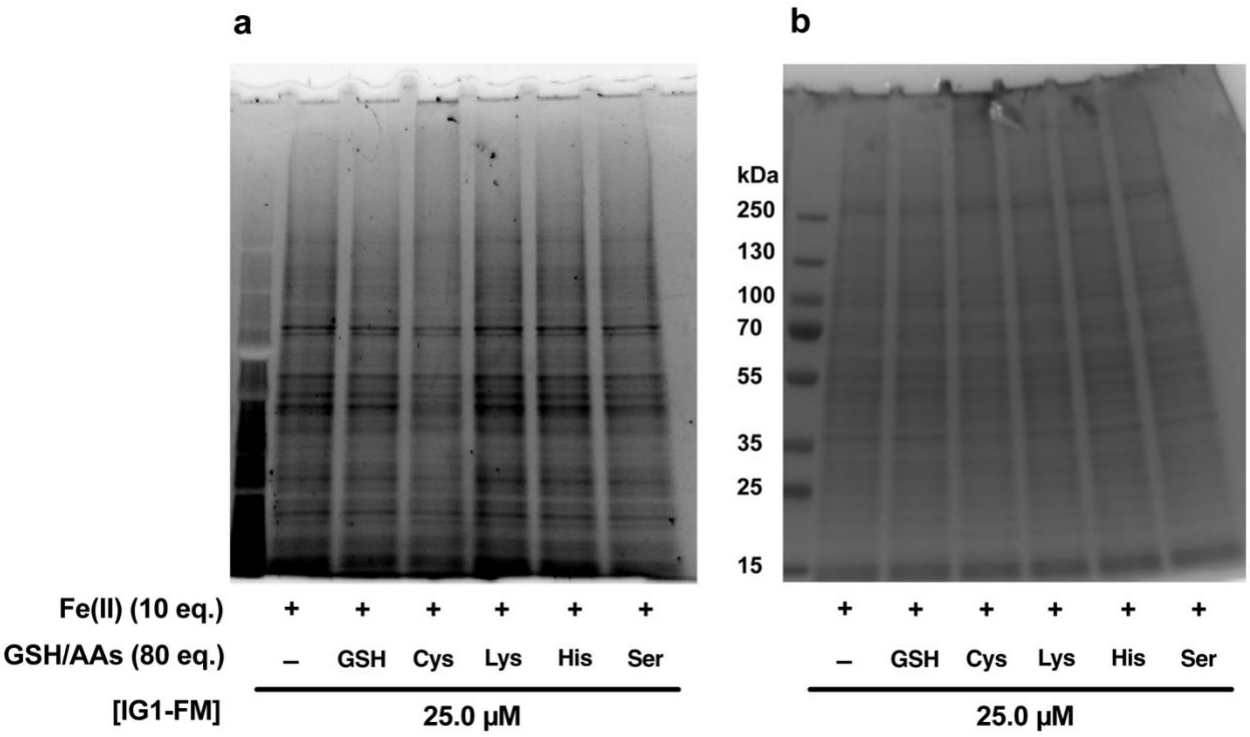

Figure S10. Full images of SDS–PAGE analysis on HEPG2 cell lysate treated with 25 μM **IG1-FM** with 10 equivalents of Fe(II), and 80 equivalents of GSH or various nucleophilic amino acids. (a) Protein labeling by **IG1-FM**, as measured by in-gel fluorescence. (b) HEPG2 cell lysate concentration, as measured by Coomassie Stain.

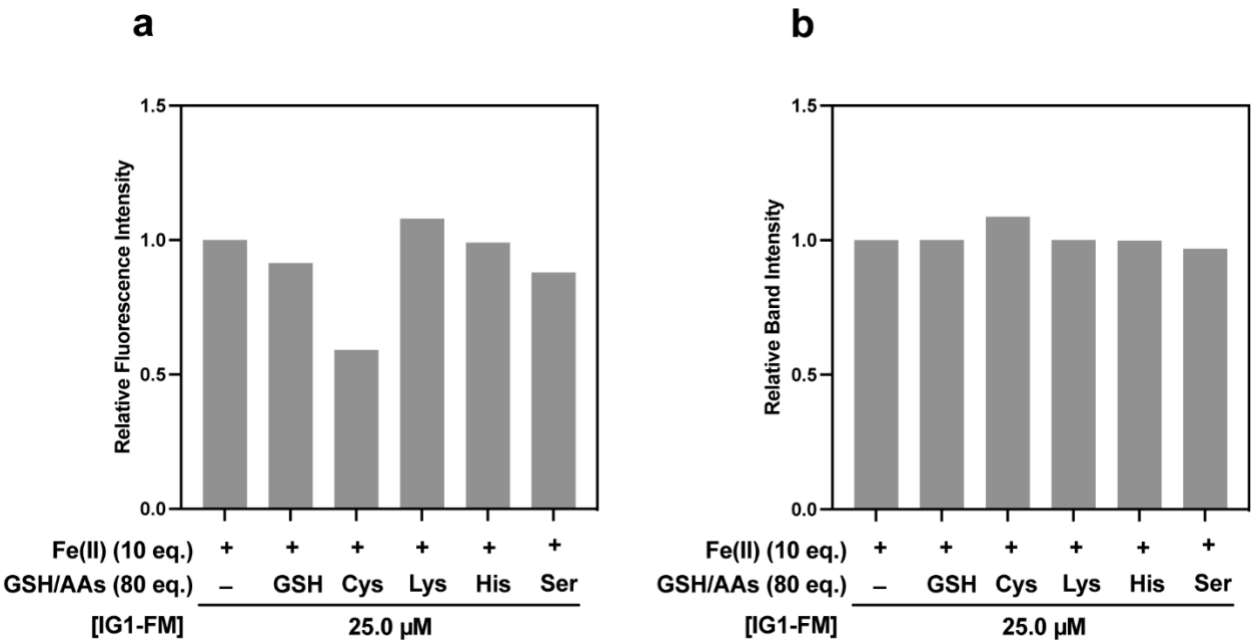

Figure S11. Competition labeling assay with **IG1-FM** and various biologically relevant nucleophiles in HEPG2 cell lysate. (a) Quantified fluorescence intensities of HEPG2 cell lysate treated with **IG1-FM**, Fe(II), and excess GSH or various nucleophilic amino acids (AAs). A solution of HEPG2 cell lysate (1.0 mg/mL) and **IG1-FM** (25 μM) in 50 mM HEPES (pH 7.4) was incubated with Fe(II) (10 eq.) and GSH or AAs (80 eq.) for 2 h. Protein labeling was measured by total lane fluorescence intensity. (b) Quantified concentration of HEPG2 cell lysate, as measured by Coomassie stain. In-gel fluorescence/intensity for SDS-PAGE was scanned by ChemiDoc MP and signal intensity was analyzed by Image Lab.

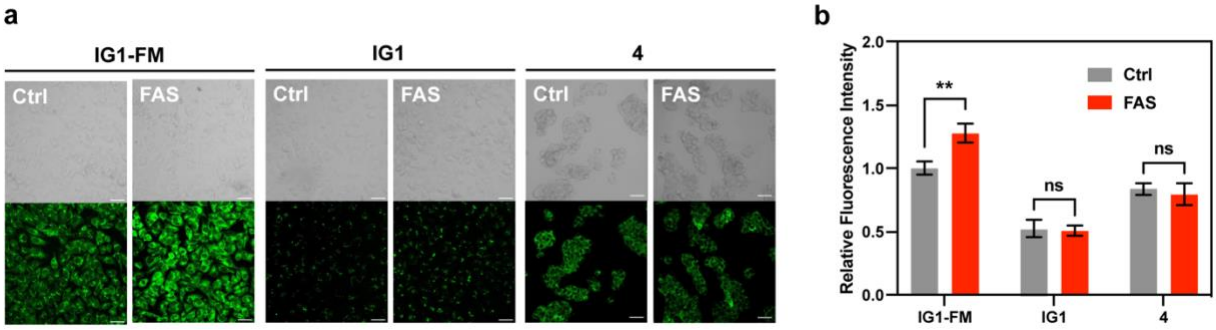

Figure S12. IG1-FM exhibits greater cellular retention than **IG1**. (a) Confocal fluorescence microscopy images of HEPG2 cells incubated with vehicle control or 100 µM FAS in low glucose DMEM/10% FBS for 90 min. Cells were then washed once with HBSS (+Ca, Mg), followed by incubation with 5 µM **IG1-FM**, **IG1**, or compound **4** in HBSS (+Ca, Mg) for 1 h. Cells were then washed twice with HBSS (+Ca, Mg) and imaged. (b) Normalized cellular fluorescence intensities of HEPG2 cells as determined using ImageJ, showing increases in fluorescence signal in response to FAS for **IG1-FM** only. Fluorescence intensity was determined from experiments performed in triplicate with λ_{ex} = 488 nm (laser settings were kept consistent between all three probes). Error bars denote standard deviation (SD; n = 3). Scale bar = 50 µm. ns, not statistically significant and **$p < 0.01$.

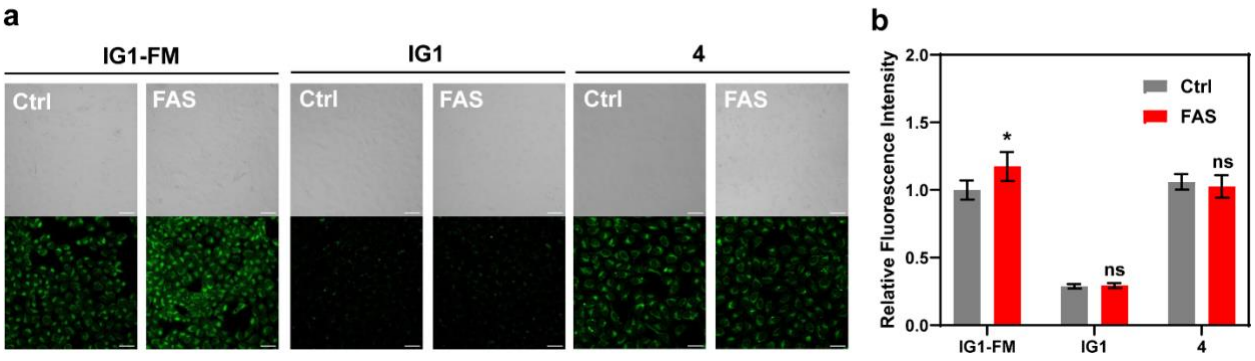

Figure S13. (a) Confocal fluorescence microscopy images of U2OS cells incubated with vehicle control or 100 µM FAS in DMEM/10% FBS for 90 min. Cells were then washed once with HBSS (+Ca, Mg), followed by incubation with 5 µM **IG1-FM**, **IG1**, or compound **4** in HBSS (+Ca, Mg) for 1 h. Cells were then washed once with HBSS (+Ca, Mg) and imaged. (b) Normalized cellular fluorescence intensities of U2OS cells as determined using ImageJ, showing increases in fluorescence signal in response to FAS for **IG1-FM** only. Fluorescence intensity was determined from experiments performed in triplicate with λ_{ex} = 488 nm (laser settings were kept consistent between all three probes). Error bars denote SD (n = 3). Scale bar = 50 µm. ns, not statistically significant and *p < 0.1.

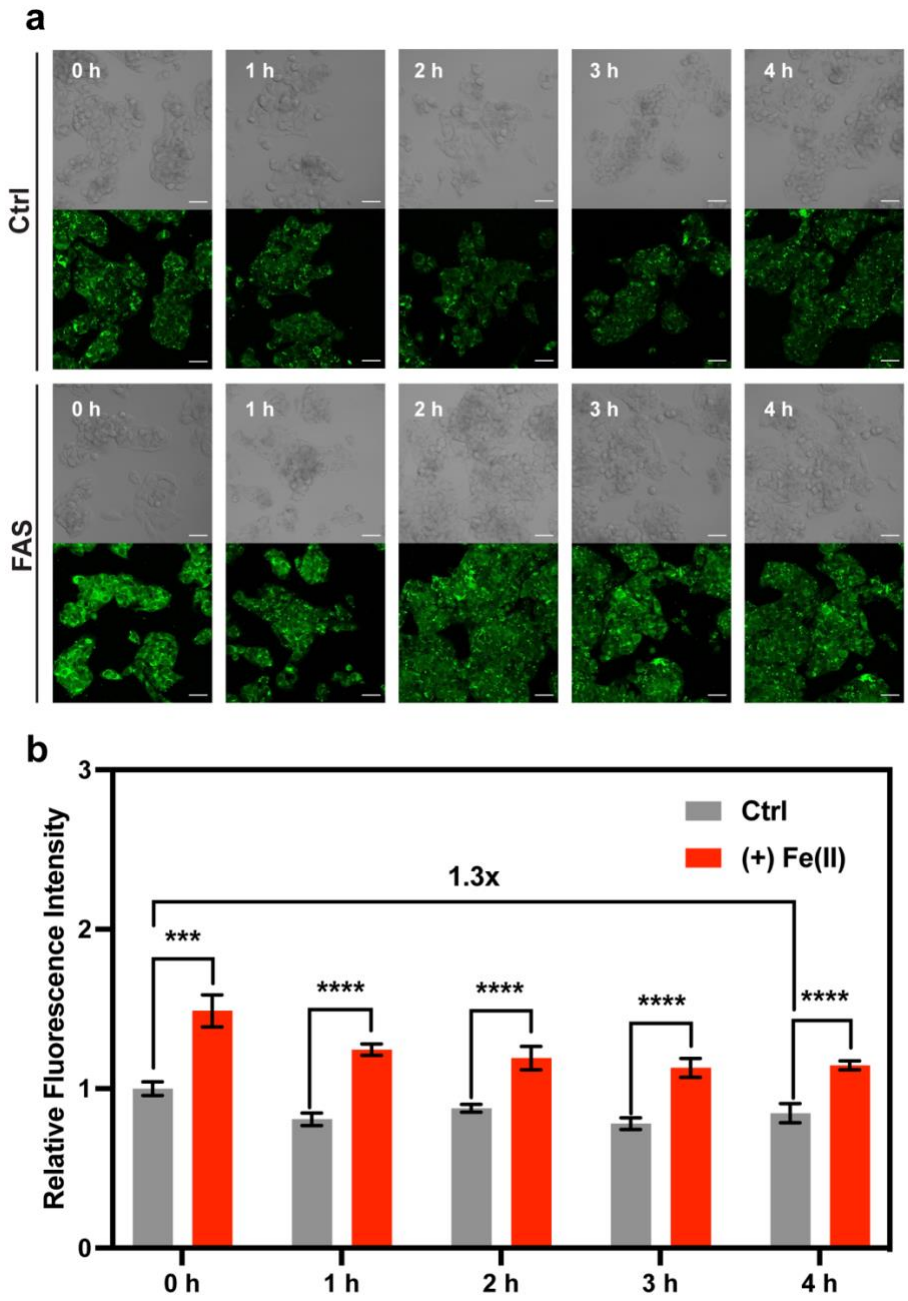

Figure S14. Time course cellular retention of **IG1-FM**. (a) Confocal fluorescence microscopy images of HEPG2 cells incubated with vehicle control or 100 µM FAS in low glucose DMEM/10% FBS for 90 min. Cells were then washed once with HBSS (+Ca, Mg), followed by incubation with 5 µM **IG1-FM** in HBSS (+Ca, Mg) for 1 h. Cells were then washed with HBSS (+Ca, Mg) (3x) and imaged every hour. (b) Normalized cellular fluorescence intensities of HEPG2 cells as determined using ImageJ, showing higher fluorescence signal for FAS treated cells over 4 hours, and minimal loss of signal over time. Fluorescence intensity was determined from experiments performed in quadruplet with λ_{ex} = 488 nm. Error bars denote SD (n = 4). Scale bar = 50 µm. ***P < 0.001, ****P < 0.0001.

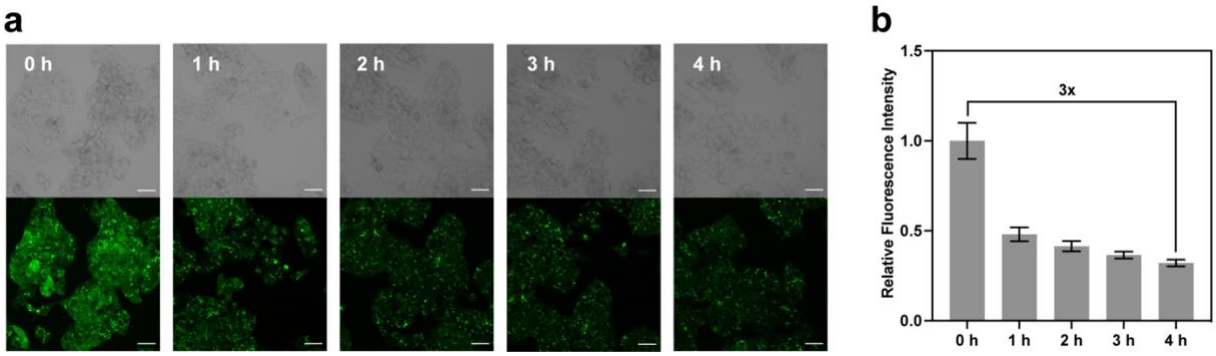

Figure S15. Time course cellular retention of **3-O-Methylfluorescein**. (a) Confocal fluorescence microscopy images of HEPG2 cells stained with **3-O-Methylfluorescein**. Cells were washed once with HBSS (+Ca, Mg), followed by incubation with 5 μM **-O-Methylfluorescein** in HBSS (+Ca, Mg) for 1 h. Cells were then washed with HBSS (+Ca, Mg) (3x) and imaged every hour. (b) Normalized cellular fluorescence intensities of HEPG2 cells as determined using ImageJ, showing significant loss of signal over time. Fluorescence intensity was determined from experiments performed in quadruplet with λ_{ex} = 488 nm. Error bars denote SD (n = 4). Scale bar = 50 μm.

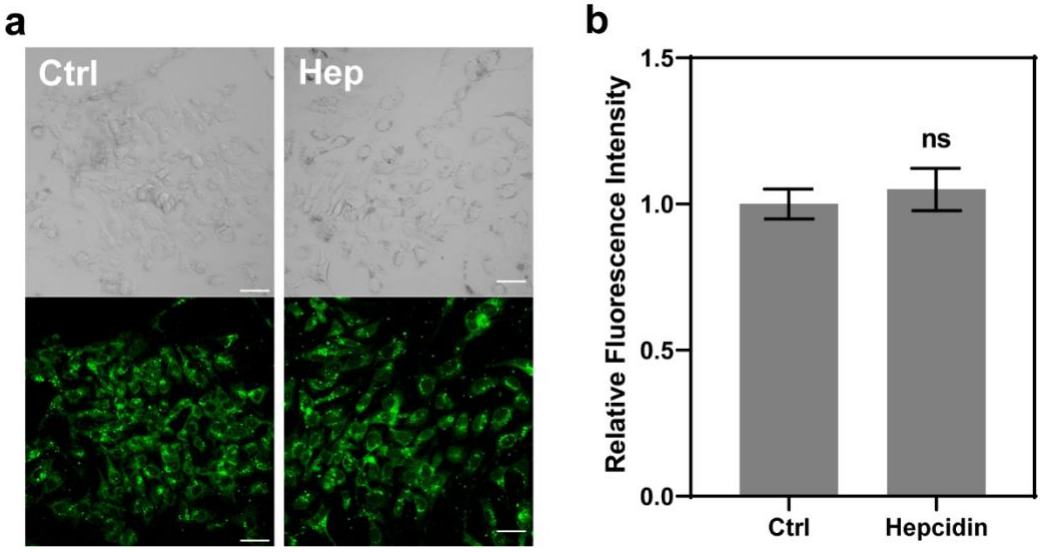

Figure S16. IG1-FM detects no changes in labile Fe in live HEPG2 cells in response to treatment with hepcidin alone. (a) Confocal microscopy images of HEPG2 cells stained with **IG1-FM** and treated with vehicle control, or Hepcidin. Cells were incubated with vehicle control or 4 μg/mL hepcidin in low glucose DMEM/10% FBS for 24 h. Cells were then washed once with HBSS (+Ca, Mg) and incubated with 5 μM **IG1-FM** in HBSS for 1 h. Finally, cells were washed twice with HBSS, and then imaged. (b) Normalized cellular fluorescence intensities of HEPG2 cells as determined using ImageJ, showing no detectable changes in signal upon treatment with hepcidin. Fluorescence intensity of **IG1-FM** was determined from experiments performed in triplicate with λ_{ex} = 488 nm. Error bars denote SD (n = 3). Scale bar = 50 μm. ns, not statistically significant.

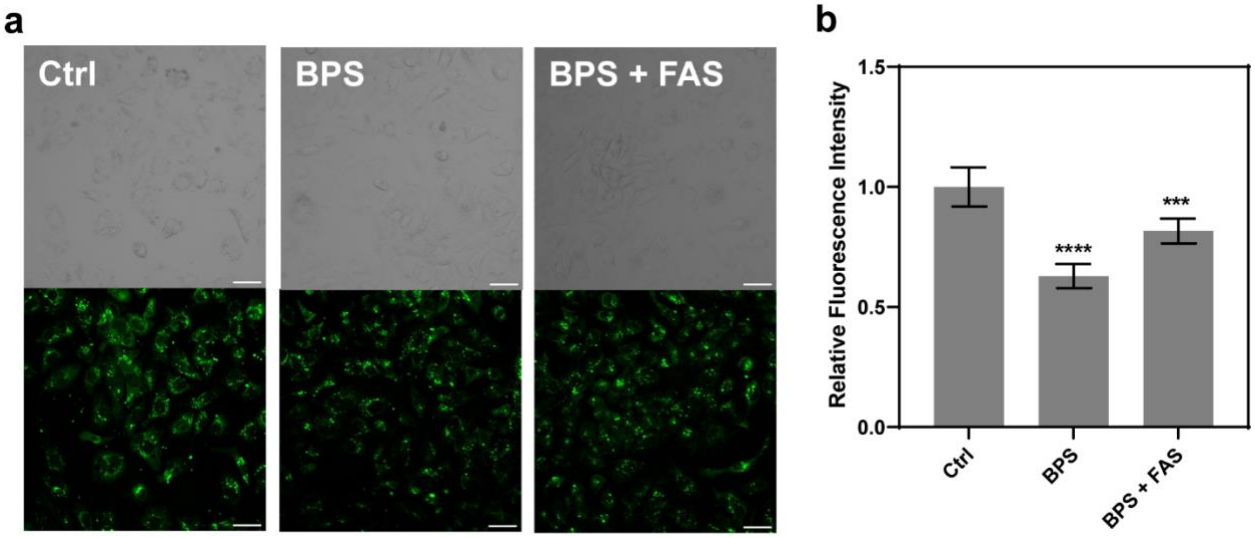

Figure S17. IG1-FM can detect decreases in labile Fe in live HEPG2 cells in response to treatment with Fe chelator BPS. (a) Confocal microscopy images of HEPG2 cells stained with **IG1-FM** and treated with vehicle control, BPS for endogenous Fe chelation, or BPS and FAS for exogenous Fe chelation. Cells were incubated with vehicle control or 1 mM BPS in low glucose DMEM/10% FBS for 24 h. Medium was then replaced with vehicle control or 100 μM FAS in low glucose DMEM/10% FBS for 90 min, washed once with HBSS (+Ca, Mg) and incubated with 5 μM **IG1-FM** in HBSS for 1 h. Finally, cells were washed twice with HBSS, and then imaged. (b) Normalized cellular fluorescence intensities of HEPG2 cells as determined using ImageJ, showing a decrease in signal upon treatment with BPS or BPS with FAS. Fluorescence intensity of **IG1-FM** was determined from experiments performed in triplicate with λ_{ex} = 488 nm. Error bars denote SD (n = 3). Scale bar = 50 μm. ***P < 0.001, ****P < 0.0001.

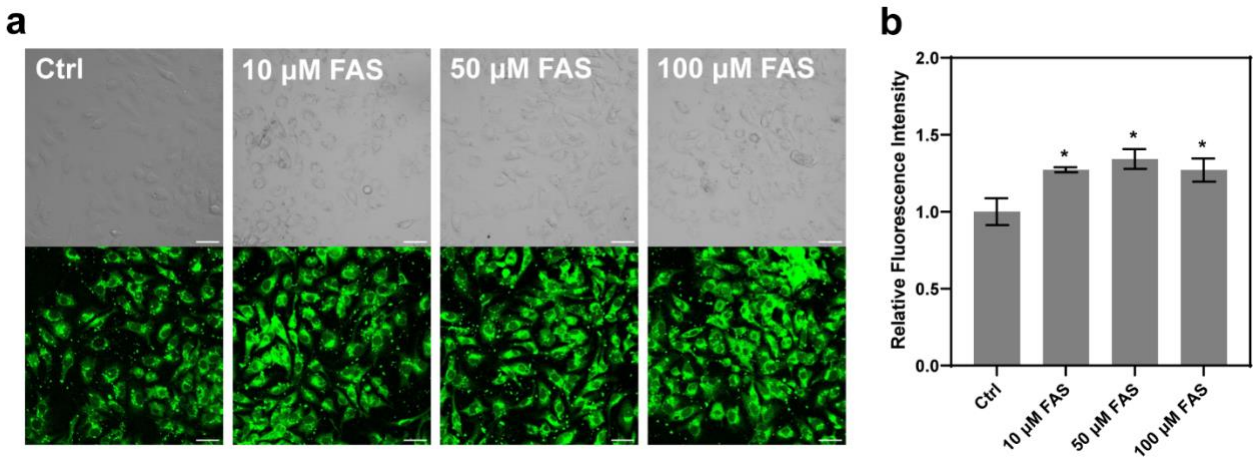

Figure S18. IG1-FM can detect increases in exogenous labile Fe in live HEPG2 cells in response to treatment with ferrous ammonium sulfate (FAS). (a) Confocal fluorescence microscopy images of HEPG2 cells incubated with vehicle control or 10-100 µM FAS in low glucose DMEM/10% FBS for 90 min. Cells were then washed once with HBSS (+Ca, Mg), followed by incubation with 10 µM **IG1-FM** in HBSS (+Ca, Mg) for 1 h. Cells were then washed twice with HBSS (+Ca, Mg) and imaged. (b) Normalized cellular fluorescence intensities of HEPG2 cells as determined using ImageJ, showing increases in fluorescence signal in response to varying concentrations of FAS. Fluorescence intensity of **IG1-FM** was determined from experiments performed in duplicate with λ_{ex} = 488 nm. Error bars denote standard deviation (SD; n = 2). Scale bar = 50 µm. *p < 0.1.

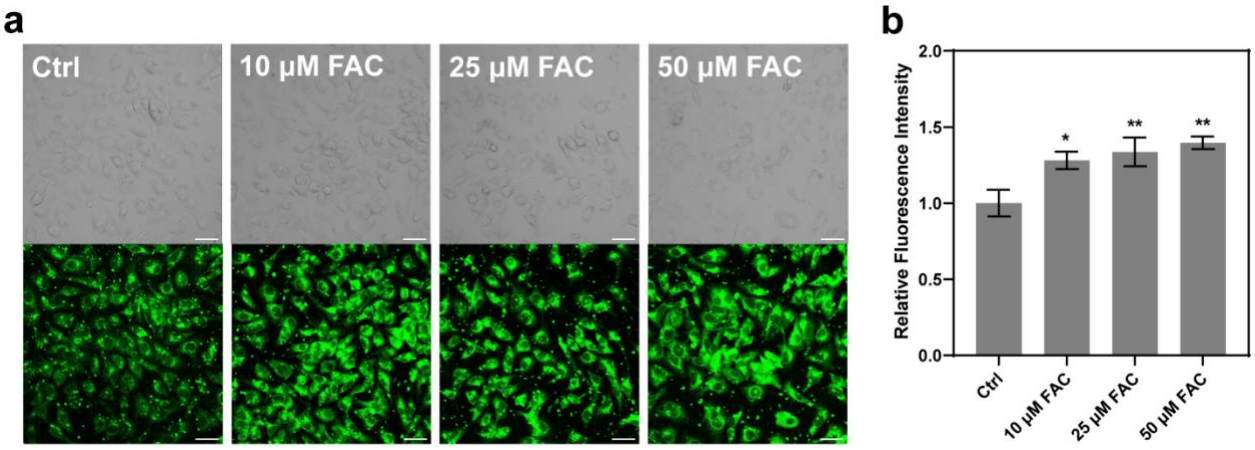

Figure S19. IG1-FM can detect increases in exogenous labile Fe in live HEPG2 cells in response to treatment with ferric ammonium citrate (FAC). (a) Confocal fluorescence microscopy images of HEPG2 cells incubated with vehicle control or 10-50 µM FAC in low glucose DMEM/10% FBS for 90 min. Cells were then washed once with HBSS (+Ca, Mg), followed by incubation with 10 µM **IG1-FM** in HBSS (+Ca, Mg) for 1 h. Cells were then washed twice with HBSS (+Ca, Mg) and imaged. (b) Normalized cellular fluorescence intensities of HEPG2 cells as determined using ImageJ, showing increases in fluorescence signal in response to varying concentrations of FAC. Fluorescence intensity of **IG1-FM** was determined from experiments performed in duplicate with λ_{ex} = 488 nm. Error bars denote standard deviation (SD; n = 2). Scale bar = 50 µm. *$p < 0.1$, **$p < 0.01$.

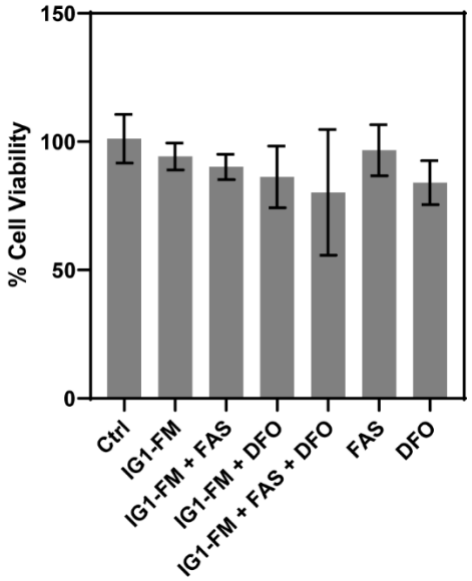

Figure S20. HEPG2 cell viability remains high in the presence of **IG1-FM** and other pharmacological treatments. Cells were incubated with vehicle control, or DFO in low glucose DMEM/10% FBS for 24 h. Medium was then replaced with vehicle control or FAS in low glucose DMEM/10% FBS for 90 min, washed once with HBSS (+Ca, Mg), incubated with **IG1-FM** in HBSS for 1 h, washed twice with HBSS, and then incubated with Hoechst 33342 for 15 min. Fluorescence was then read on a plate reader (monofilter) with λ_{ex} = 350 nm (9 mm bandwidth), λ_{em} = 460 (9 mm bandwidth), 15 mm plate height and top-down fluorescence detection. Error bars denote SD.

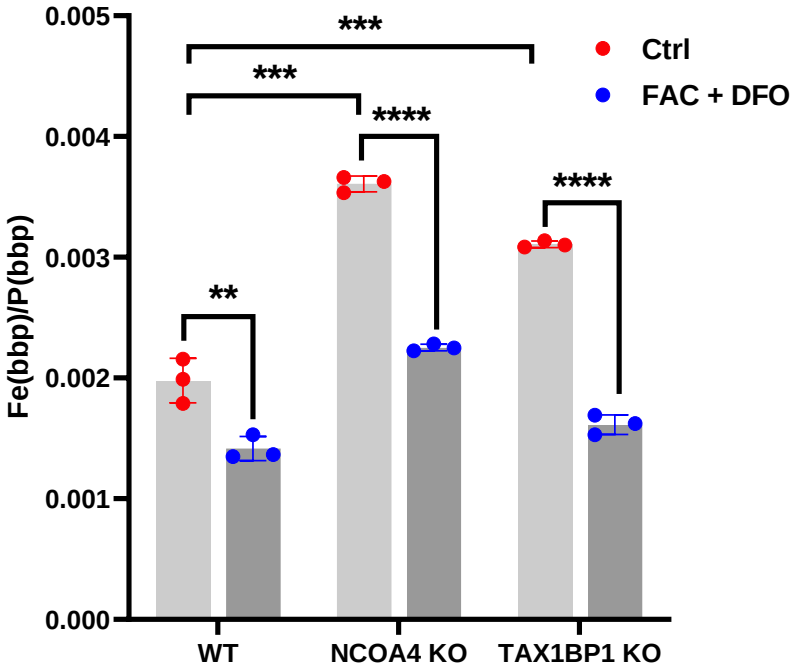

Figure S21. ICP−MS measurements of total cellular ^{56}Fe levels in WT HeLa cells with or without NCOA4 KO or TAX1BP1 KO treated with vehicle control or FAC and DFO. Cells were incubated with vehicle control or 50 μM FAC in DMEM/10% FBS for 24 h. Medium was then replaced with vehicle control or 100 μM DFO in DMEM/10% FBS for 24 h. HeLa cells with NCOA4 KO or TAX1BP1 KO have elevated levels of total iron versus WT cells, and cells treated with FAC and DFO had diminished levels of total iron versus untreated cells. Normalization of different cell numbers is obtained by total cellular ^{31}P level. Error bars denote SD (n = 3). **P < 0.01, ***P < 0.001, ****P < 0.0001.

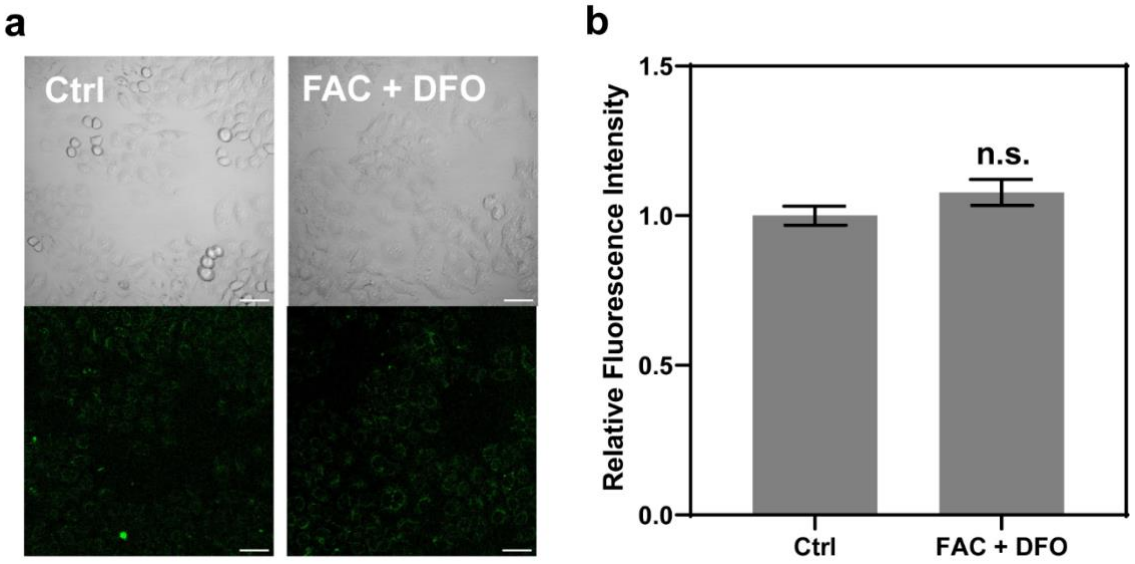

Figure S22. IG1 is unable to detect changes in labile Fe in live HeLa cells in response to treatment with FAC and DFO. (a) Confocal microscopy images of wildtype (WT) HeLa cells stained with **IG1**. Cells were incubated with vehicle control or 50 μM FAC in DMEM/10% FBS for 24 h. Medi was then replaced with vehicle control or 100 μM DFO in DMEM/10% FBS for 24 h, washed once with HBSS (+Ca, Mg), incubated with 5 μM **IG1** in HBSS for 1 h, and then imaged. (b) Normalized cellular fluorescence intensities of HeLa cells as determined using ImageJ, showing no changes in fluorescence signal in response to FAC and DFO. Fluorescence intensity of **IG1** was determined from experiments performed in triplicate with λ_{ex} = 488 nm. Error bars denote SD (n = 3). Scale bar = 50 μm. ns, not statistically significant.

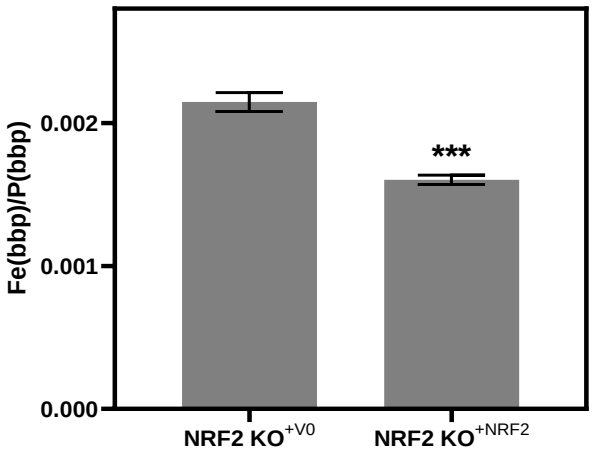

Figure S23. ICP−MS measurements of total cellular ^{56}Fe levels in of A549 cells stably expressing NRF2 knockout (NRF2 KO^{+V0}) or NRF2 knockout with genetic rescue (NRF2 KO^{+NRF2}), showing decreases in total iron upon reintroduction and activation of NRF2. Normalization of different cell numbers is obtained by total cellular ^{31}P level. Error bars denote SD (n = 3). ***P < 0.001.

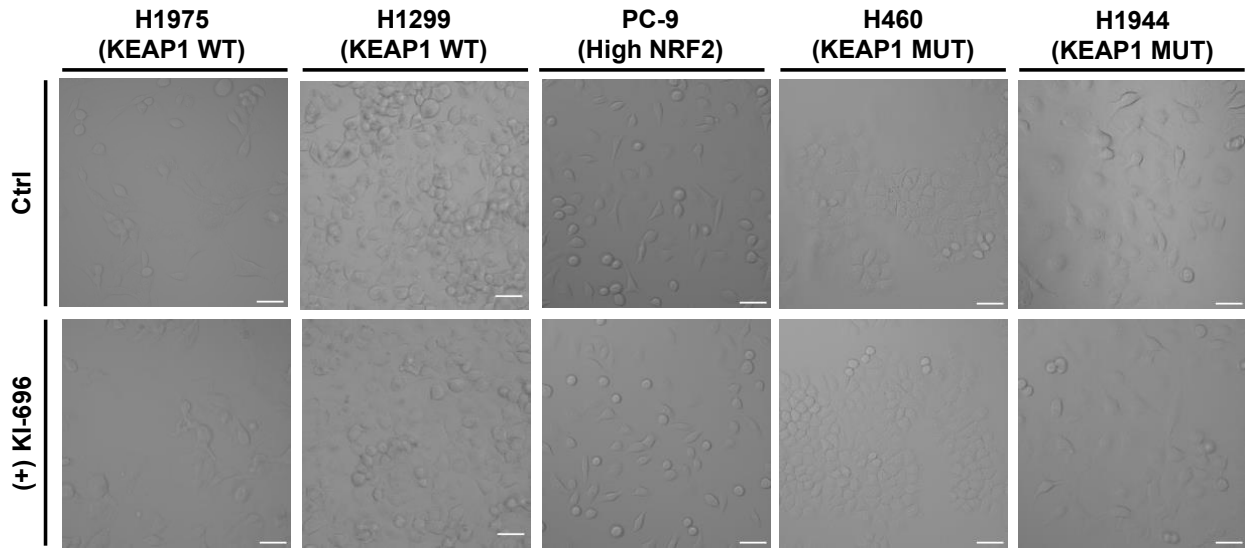

Figure S24. Brightfield images of **IG1-FM**-stained NSCLC cell lines with wildtype KEAP1 (KEAP1 WT), wildtype KEAP1 and high levels of NRF2 (High NRF2), or mutant KEAP1 (KEAP1 MUT), treated with and without a KEAP1 inhibitor (KI-696). Scale bar = 50 μm.

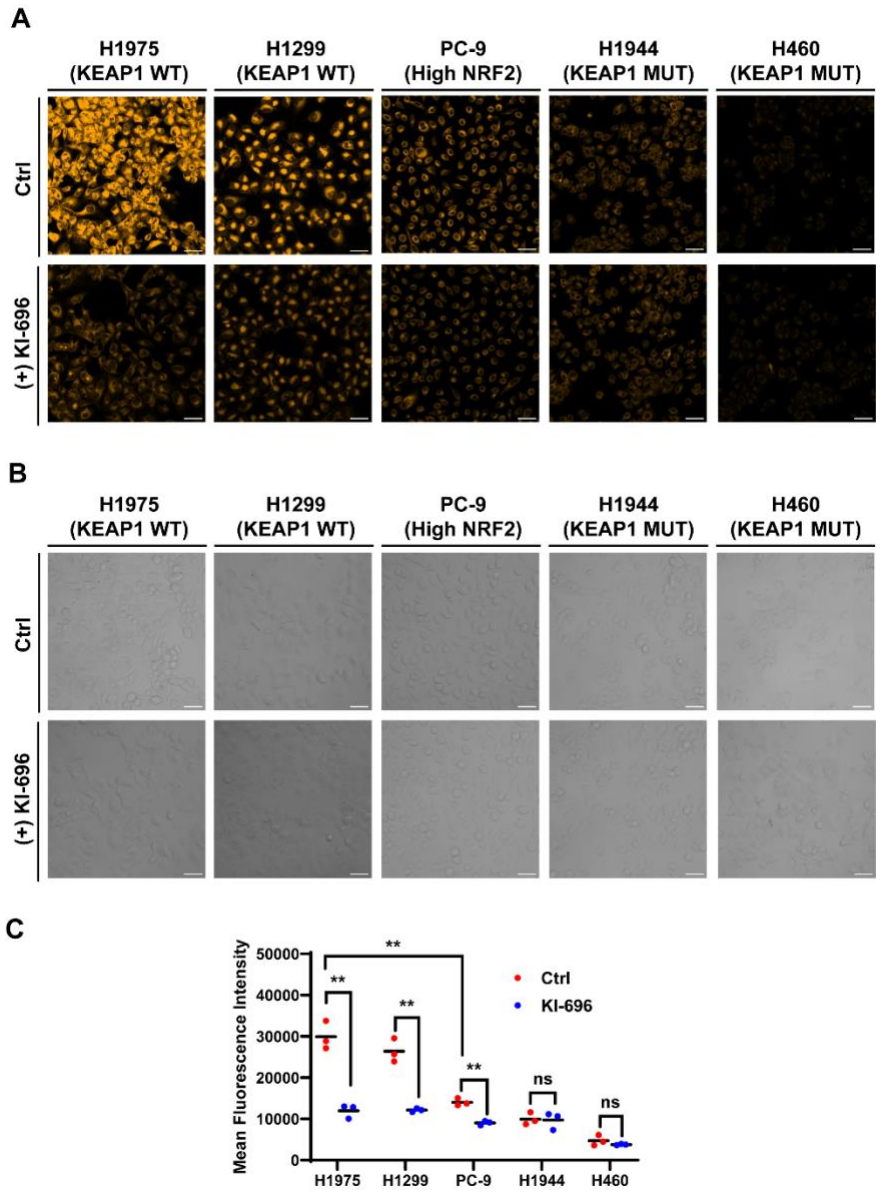

Figure S25. (A) Confocal fluorescence images of **RhoNox-4** in NSCLC cell lines with wildtype KEAP1 (KEAP1 WT), wildtype KEAP1 and high levels of NRF2 (High NRF2), or mutant KEAP1 (KEAP1 MUT), treated with and without a KEAP1 inhibitor (KI-696). Cells were incubated with vehicle control or 1 μM KI-696 in RPMI 1640/10% FBS for 48 h. Cells were then washed once with HBSS and incubated with **RhoNox-4** (1 μM) in HBSS for 30 minutes. Cells were then washed twice with HBSS and imaged. (B) Brightfield images of **RhoNox-4**-stained NSCLC cells. (C) Mean **RhoNox-4** fluorescence intensity in NSCLC cells. Fluorescence intensity of **RhoNox-4** was determined from experiments performed in triplicate with λ_{ex} = 561 nm. Error bars denote SD (n = 3). Scale bar = 50 μm. **P < 0.01; ns, not statistically significant.

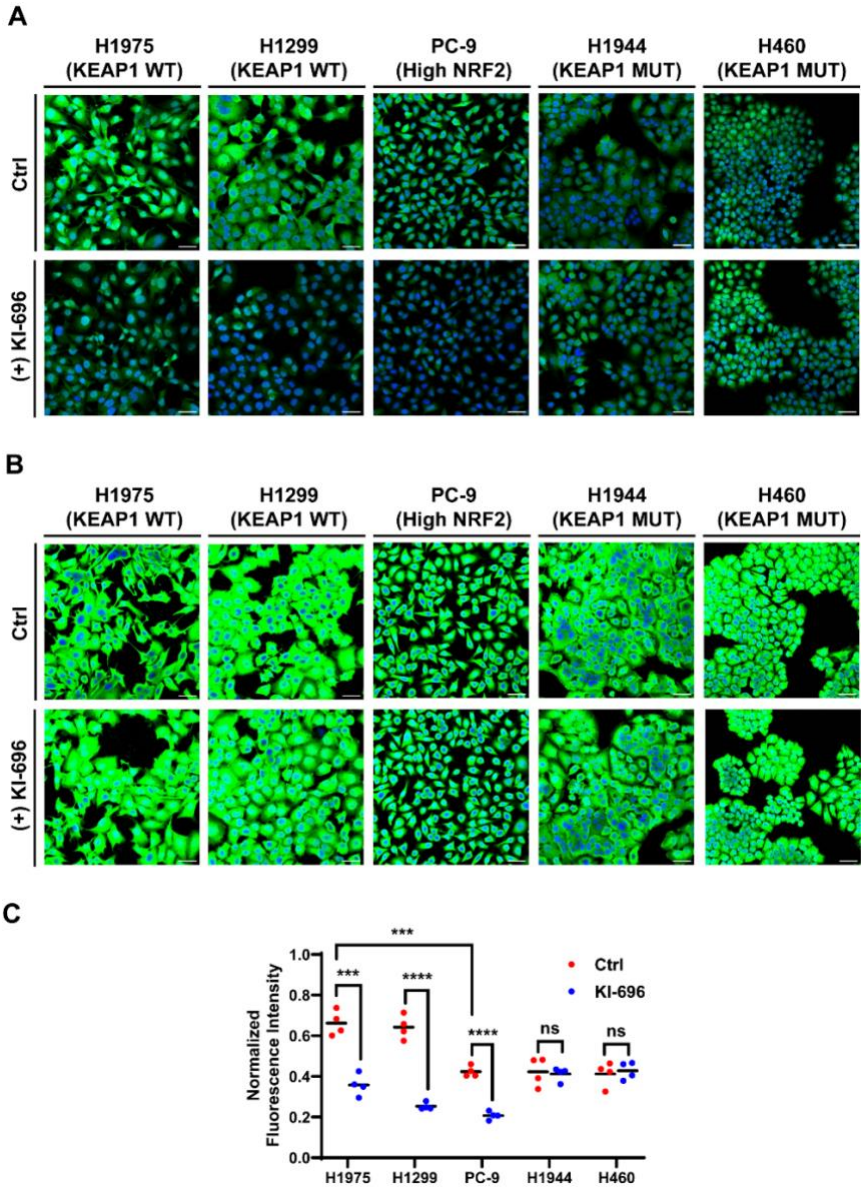

Figure S26. Confocal immunofluorescence images of (A) **TRX-Puro** or (B) free puromycin in NSCLC cell lines with wildtype KEAP1 (KEAP1 WT), wildtype KEAP1 and high levels of NRF2 (High NRF2), or mutant KEAP1 (KEAP1 MUT), treated with and without a KEAP1 inhibitor (KI-696). Cells were incubated with vehicle control or 1 μM KI-696 in RPMI 1640/10% FBS for 48 h. Cells were then washed twice with RPMI (no FBS) and incubated with **TRX-Puro** or puromycin in RPMI (no FBS) for 4 h. Cells were then fixed with 4% paraformaldehyde, immunostained with an anti-puromycin antibody, an antibody–Alexa Fluor 488 conjugate, and imaged. (C) **TRX-puro** fluorescence intensity in NSCLC cells. Green signal represents puromycin immunofluorescence and blue signal represents Hoechst 33342 fluorescence. **TRX-puro** fluorescence intensity was normalized to fluorescence intensity from free puromycin-stained cells and determined from experiments performed in quadruplet with λ_{ex} = 488 nm. Error bars denote SD (n = 4). Scale bar = 50 μm. ***P < 0.001, ****P < 0.0001; ns, not statistically significant.

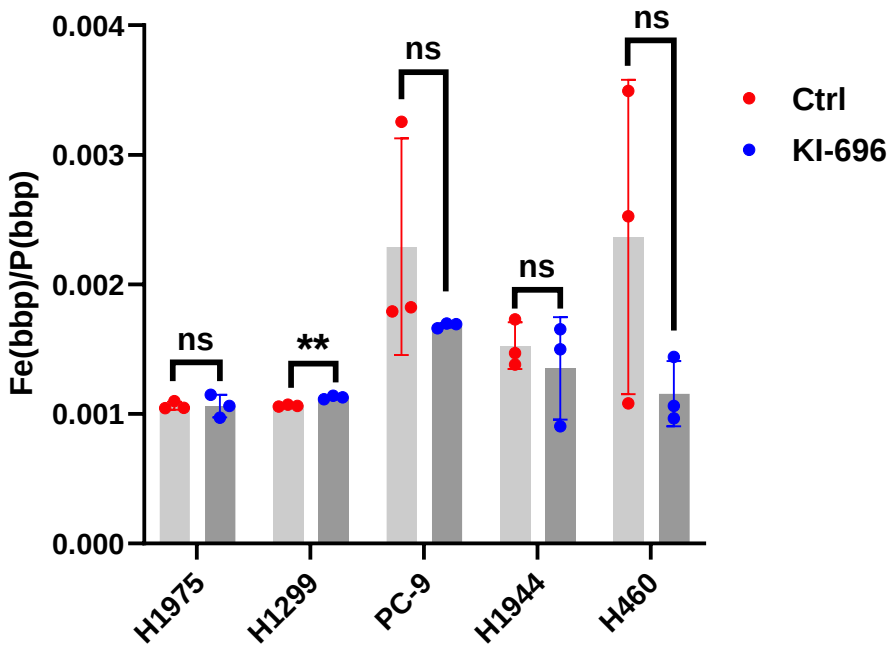

Figure S27. ICP−MS measurements of total cellular ^{56}Fe levels in NSCLC cell lines treated with or without KEAP1 inhibitor KI-696, showing no significant changes in total iron upon KI-696 treatment (aside from H1299) and no significant correlation between KEAP1 activity and total iron levels. Cells were incubated with vehicle control or 1 μM KI-696 in RPMI 1640/10% FBS for 48 h. Normalization of different cell numbers is obtained by total cellular ^{31}P level. Error bars denote SD (n = 3). **P < 0.01; ns, not statistically significant.

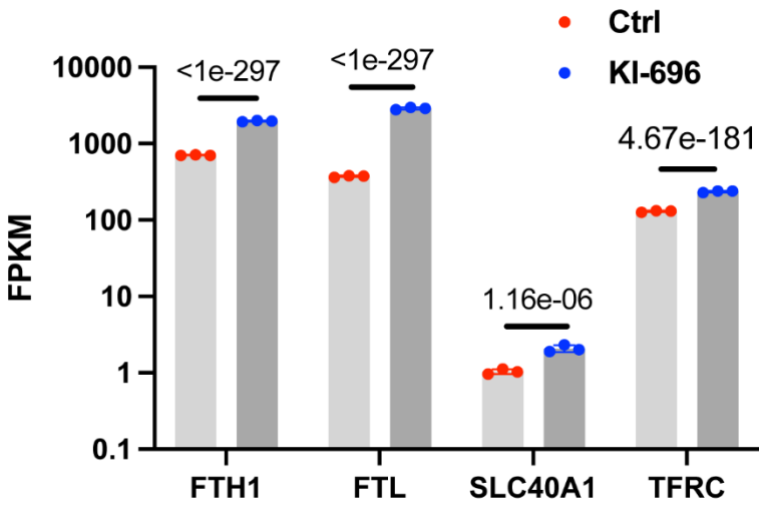

Figure S28. Expression levels of labile iron-regulating genes (FTH1, ferritin heavy chain 1; FTL, ferritin light chain; SLC40A1, ferroportin; TFRC, transferrin receptor) in H1975 cells treated with vehicle control or KEAP1 inhibitor (KI-696). Expression levels are presented as fragments per kilobase of transcript per million mapped reads (FPKM) and were determined from experiments performed in triplicate. Statistical significance is presented as adjusted p-values.

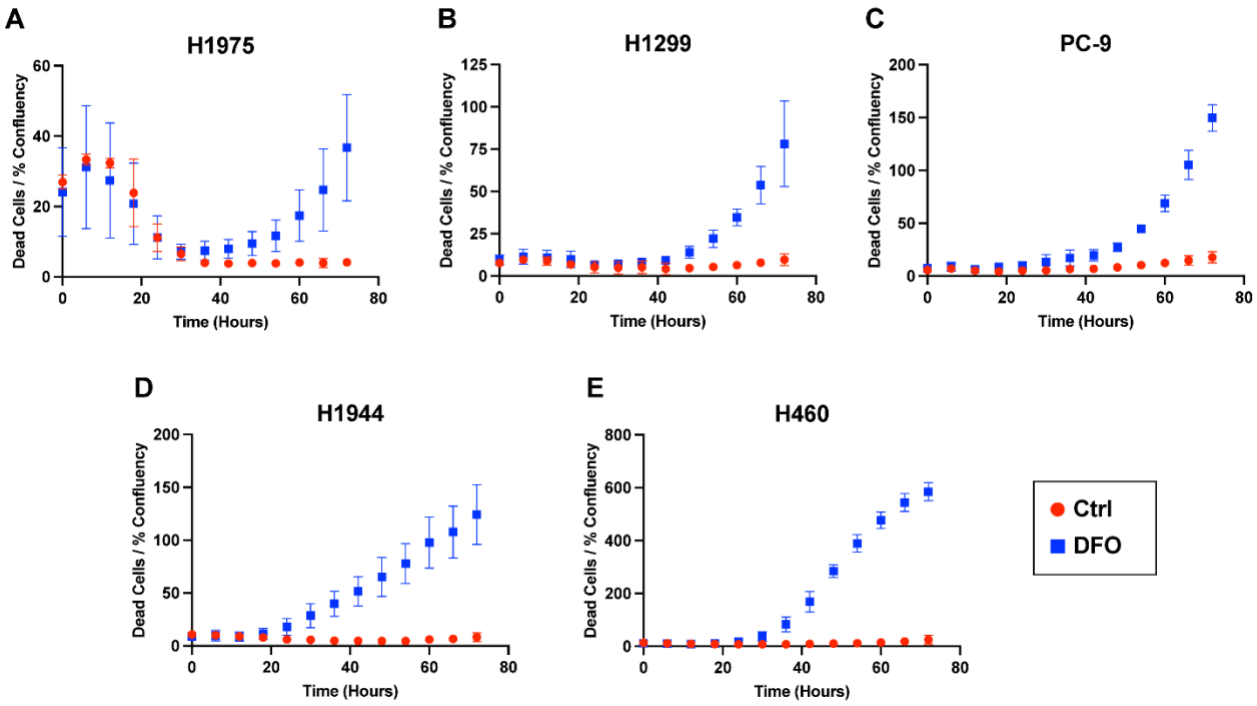

Figure S29. Cell death of NSCLC cell lines with wildtype KEAP1 (H1975 and H1299), wildtype KEAP1 and high levels of NRF2 (PC-9), or mutant KEAP1 (H1944, H460), treated with vehicle control or deferoxamine (DFO). Cells were incubated with vehicle control or 100 μM DFO in RPMI 1640/10% FBS over 72 h and cell death was monitored via Sytox Green, as previously described (2). Data were acquired with a 10X objective lens in phase contrast and green fluorescence channels (Ex/Em: 460/524 nm, acquisition time: 200 ms). Error bars denote SD (n = 3).

4. SI References

1. B. Spangler, *et al.*, A reactivity-based probe of the intracellular labile ferrous iron pool. *Nature Chemical Biology* **12**, 680–685 (2016).

2. Y. P. Kang, *et al.*, Non-canonical Glutamate-Cysteine Ligase Activity Protects against Ferroptosis. *Cell Metabolism* **33**, 174–189.e7 (2021).

3. R. L. Gonciarz, *et al.*, In vivo bioluminescence imaging of labile iron in xenograft models and liver using FeAL-1, an iron-activatable form of D-luciferin. *Cell Chemical Biology* **30**, 1468–1477.e6 (2023).

4. B. R. Blank, *et al.*, Antimalarial Trioxolanes with Superior Drug-Like Properties and In Vivo Efficacy. *ACS Infect. Dis.* **6**, 1827–1835 (2020).

5. Scans of NMR, HRMS Spectra and UPLC-MS Chromatogram

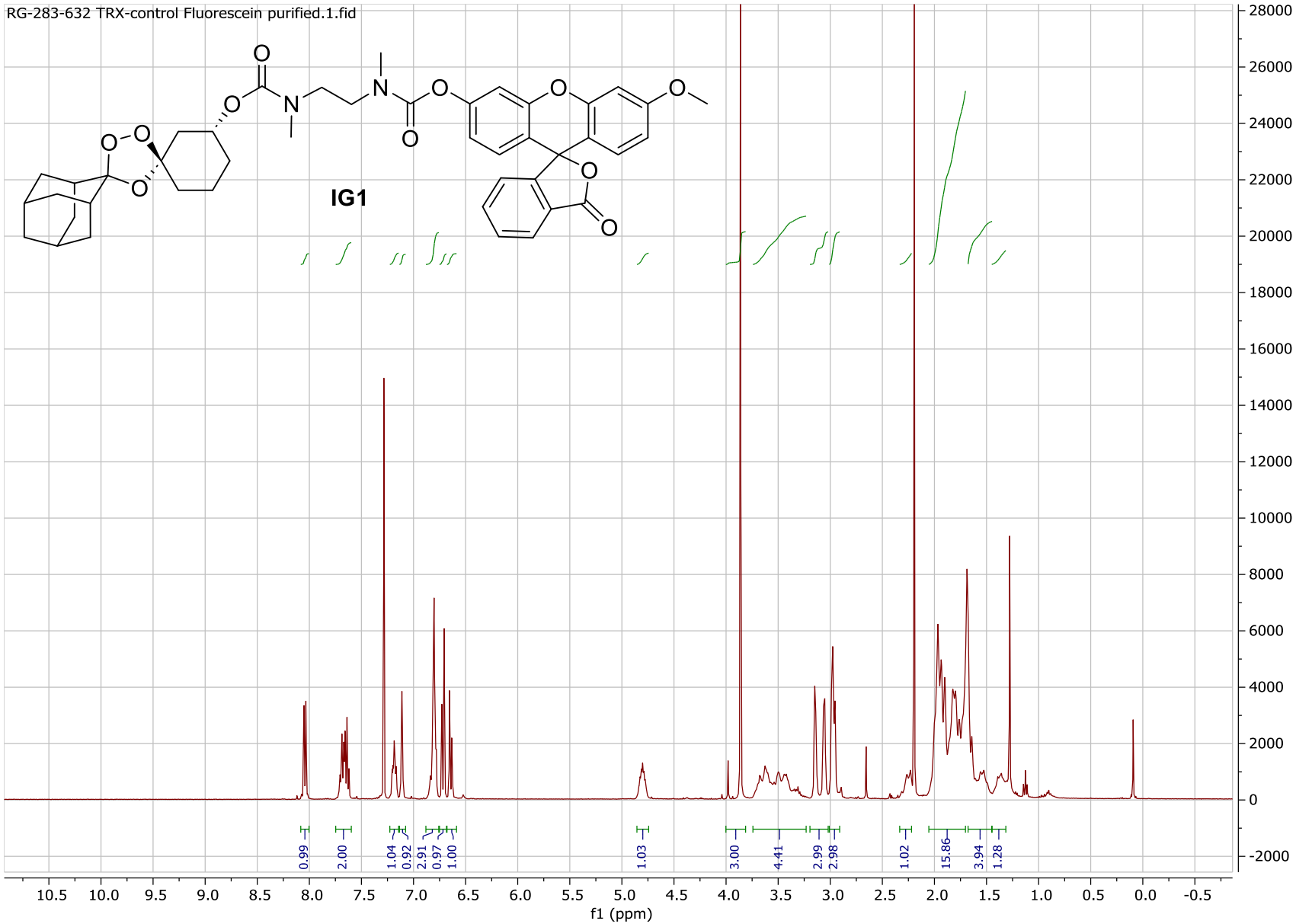
RG-283-632 TRX-control Fluorescein purified.1.fid
IG1
0.99
2.00
1.04
0.92
2.91
0.97
1.00
1.03
3.00
4.41
2.99
2.98
1.02
15.86
3.94
1.28
f1 (ppm)

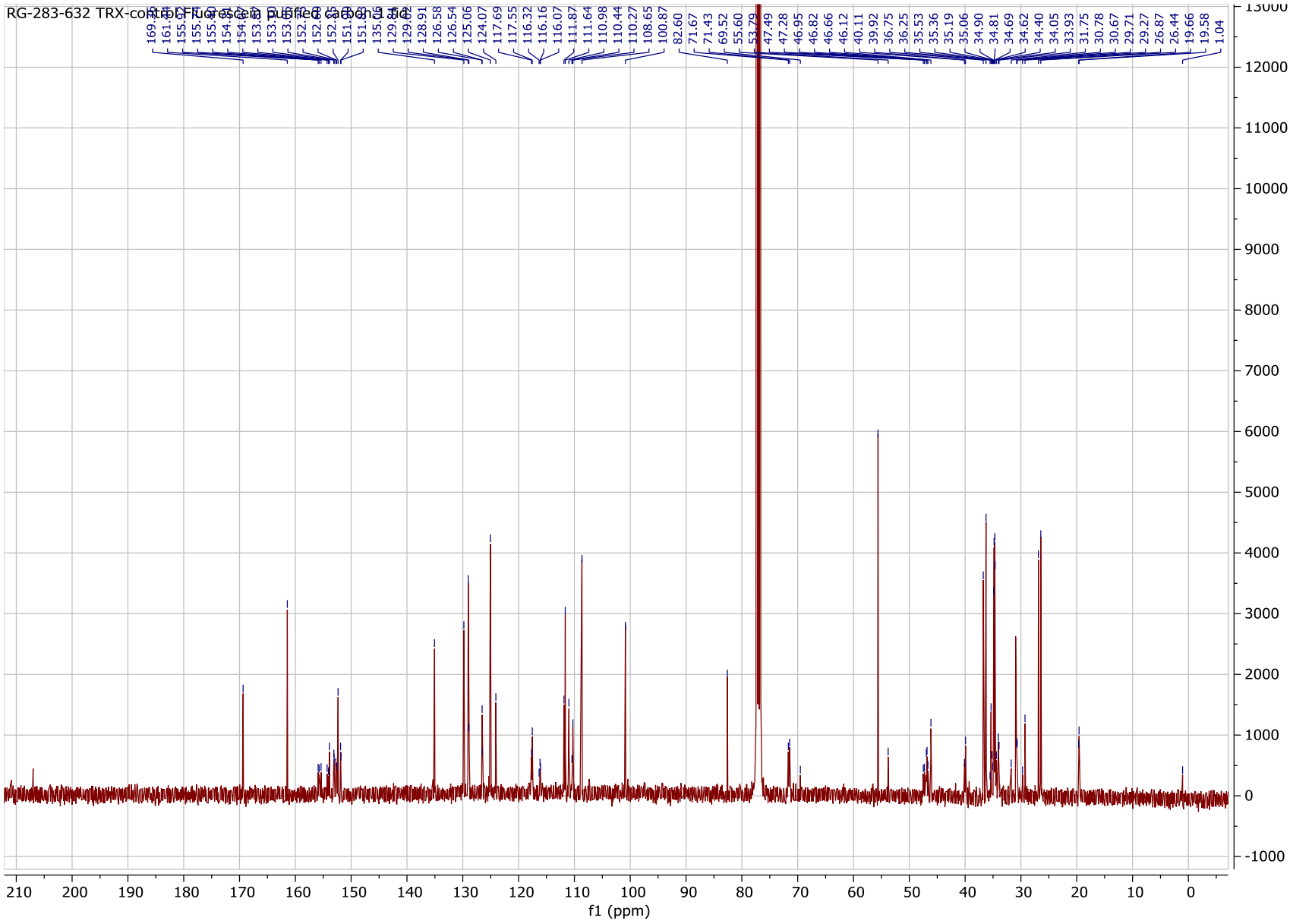
RG-283-632 TRX-control Fluorescein purified carbon 1.fid
169.
161.
155.
155.
155.
154.
154.
153.
153.
153.
152.
152.
152.
151.
151.
135.
129.
129.
128.91
126.58
126.54
125.06
124.07
117.69
117.55
116.32
116.16
116.07
111.87
111.64
110.98
110.44
110.27
108.65
100.87
82.60
71.67
71.43
69.52
55.60
53.79
47.49
47.28
46.95
46.82
46.66
46.12
40.11
39.92
36.75
36.25
35.53
35.36
35.19
35.06
34.90
34.81
34.69
34.62
34.40
34.05
33.93
31.75
30.78
30.67
29.71
29.27
26.87
26.44
19.66
19.58
1.04
13000
12000
11000
10000
9000
8000
7000
6000
5000
4000
3000
2000
1000
0
-1000
210
200
190
180
170
160
150
140
130
120
110
100
90
80
70
60
50
40
30
20
10
0
f1 (ppm)

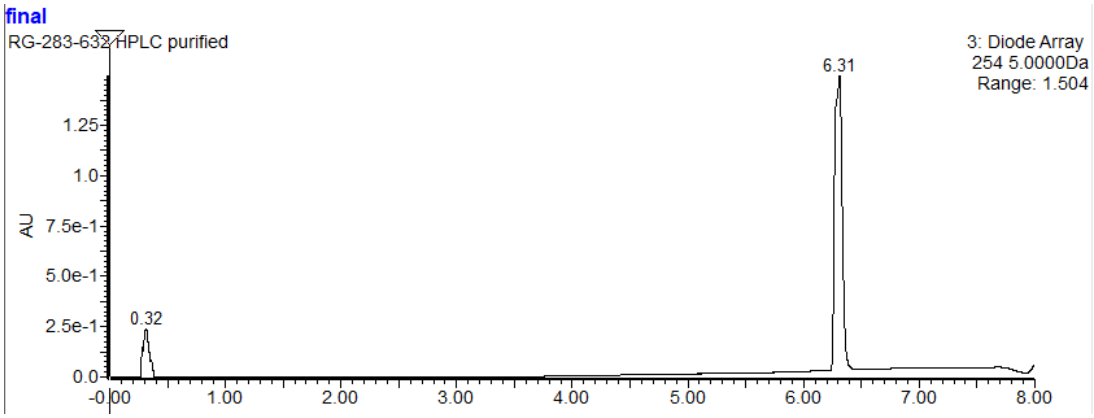
final
RG-283-632 HPLC purified
3: Diode Array
254 5.0000Da
Range: 1.504
6.31
0.32
AU
1.25
1.0
7.5e-1
5.0e-1
2.5e-1
0.0
-0.00
1.00
2.00
3.00
4.00
5.00
6.00
7.00
8.00

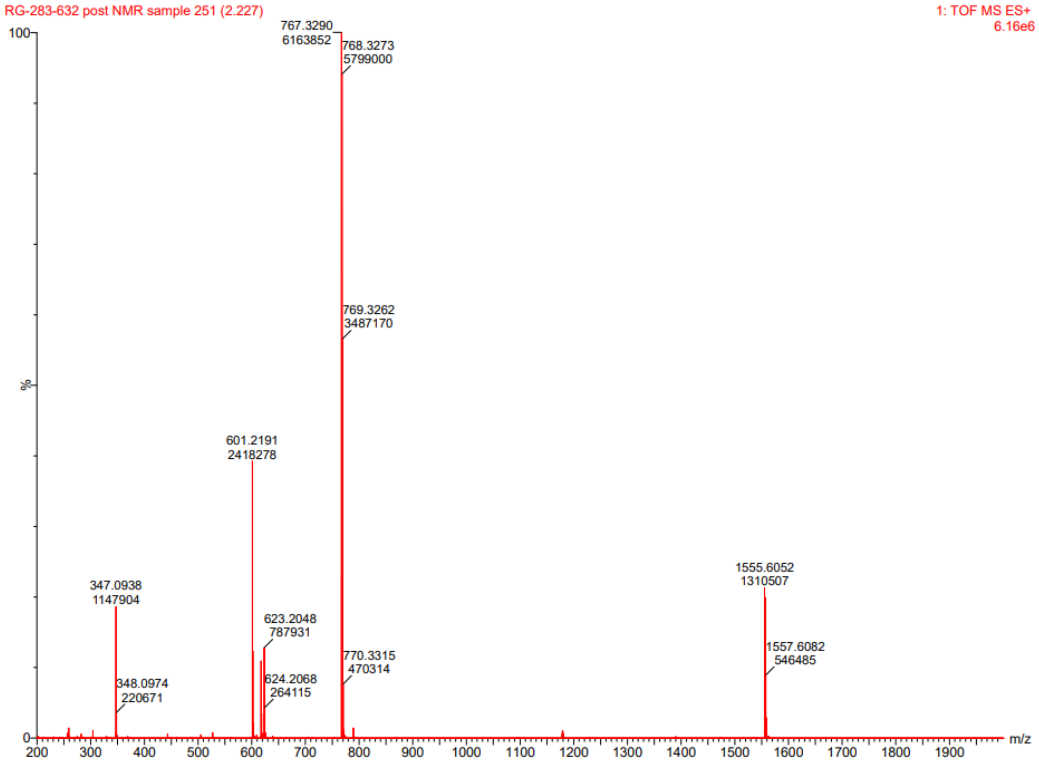
RG-283-632 post NMR sample 251 (2.227)
1: TOF MS ES+
6.16e6
100
%
0
767.3290
6163852
768.3273
5799000
769.3262
3487170
601.2191
2418278
347.0938
1147904
623.2048
787931
770.3315
470314
348.0974
220671
624.2068
264115
1555.6052
1310507
1557.6082
546485
m/z
200
300
400
500
600
700
800
900
1000
1100
1200
1300
1400
1500
1600
1700
1800
1900

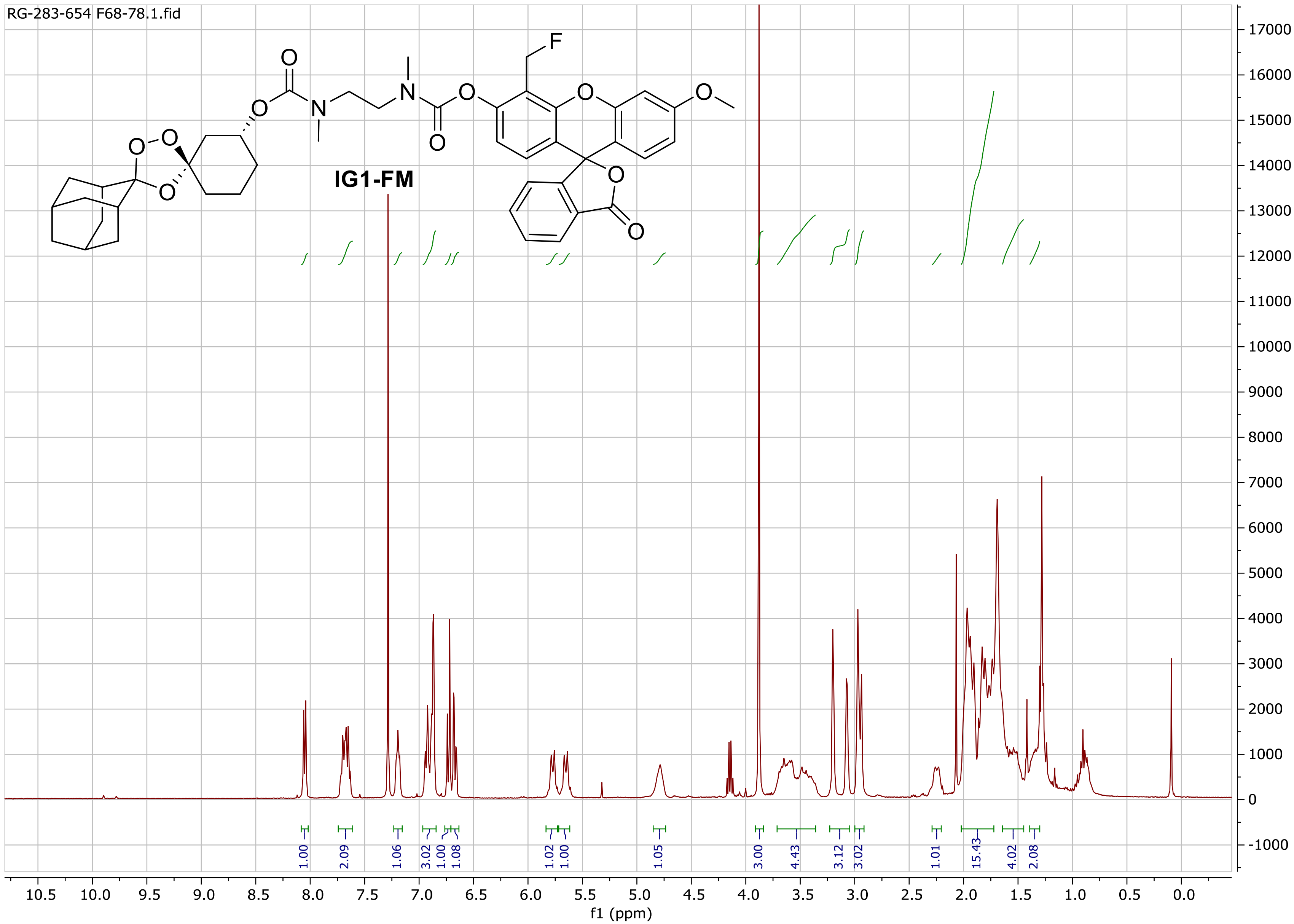
RG-283-654 F68-78.1.fid
IG1-FM
f1 (ppm)
1.00
2.09
1.06
3.02
1.00
1.08
1.02
1.00
1.05
3.00
4.43
3.12
3.02
1.01
15.43
4.02
2.08

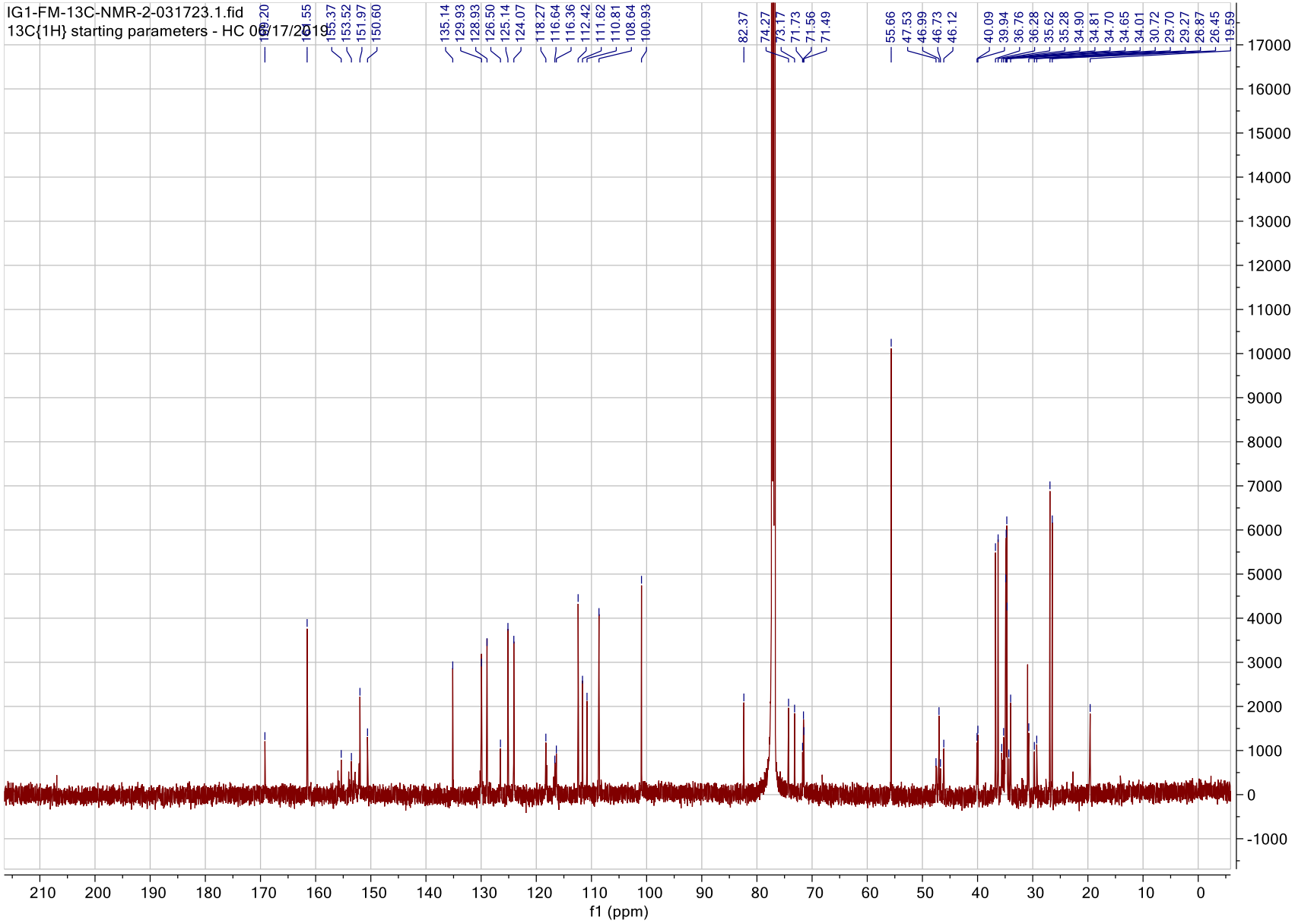
IG1-FM-13C-NMR-2-031723.1.fid
13C{1H} starting parameters - HC 06/17/2019
169.20
158.55
155.37
153.52
151.97
150.60
135.14
129.93
128.93
126.50
125.14
124.07
118.27
116.64
116.36
112.42
111.62
110.81
108.64
100.93
82.37
74.27
73.17
71.73
71.56
71.49
55.66
47.53
46.99
46.73
46.12
40.09
39.94
36.76
36.28
35.62
35.28
34.90
34.81
34.70
34.65
34.01
30.72
29.70
29.27
26.87
26.45
19.59
17000
16000
15000
14000
13000
12000
11000
10000
9000
8000
7000
6000
5000
4000
3000
2000
1000
0
-1000
210
200
190
180
170
160
150
140
130
120
110
100
90
80
70
60
50
40
30
20
10
0
f1 (ppm)

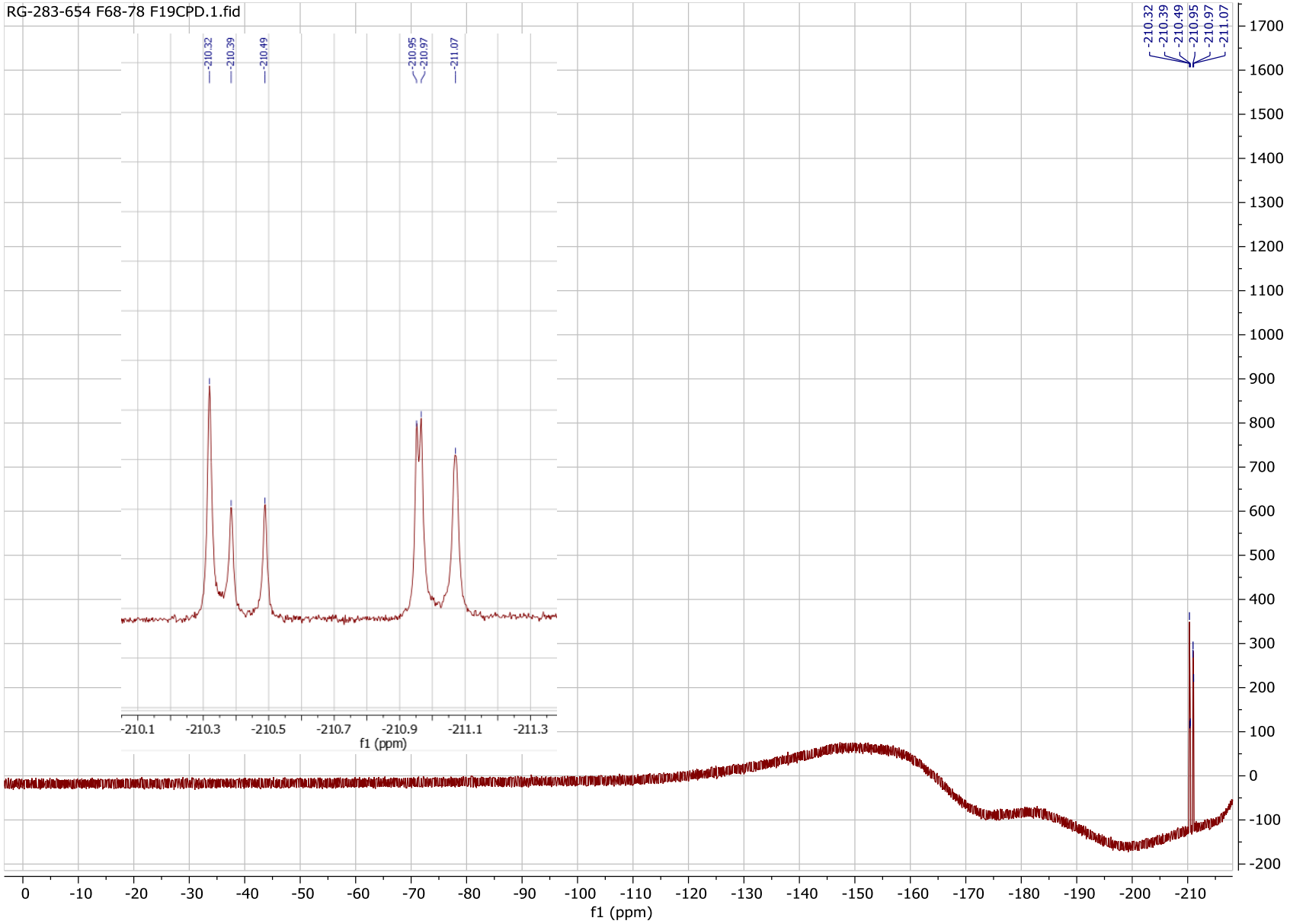
RG-283-654 F68-78 F19CPD.1.fid
-210.32
-210.39
-210.49
-210.95
-210.97
-211.07
-210.1
-210.3
-210.5
-210.7
-210.9
-211.1
-211.3
f1 (ppm)
1700
1600
1500
1400
1300
1200
1100
1000
900
800
700
600
500
400
300
200
100
0
-100
-200
0
-10
-20
-30
-40
-50
-60
-70
-80
-90
-100
-110
-120
-130
-140
-150
-160
-170
-180
-190
-200
-210
f1 (ppm)

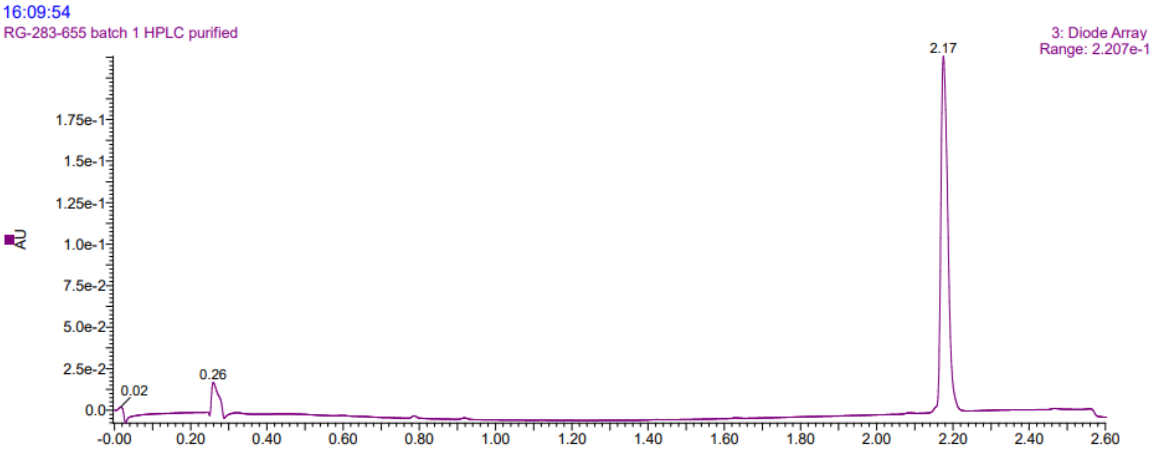
16:09:54
RG-283-655 batch 1 HPLC purified
3: Diode Array
Range: 2.207e-1
AU
2.17
0.26
0.02

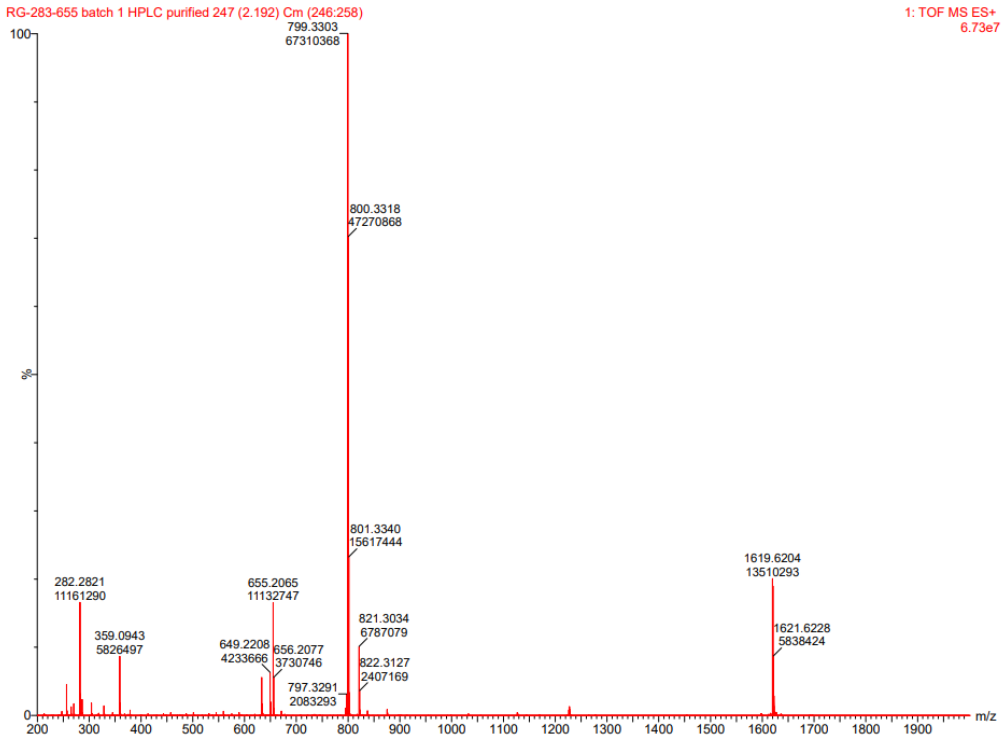
RG-283-655 batch 1 HPLC purified 247 (2.192) Cm (246:258)
1: TOF MS ES+
6.73e7
%
m/z
799.3303
67310368
800.3318
47270868
801.3340
15617444
1619.6204
13510293
282.2821
11161290
655.2065
11132747
359.0943
5826497
649.2208
4233666
656.2077
3730746
821.3034
6787079
822.3127
2407169
797.3291
2083293
1621.6228
5838424